Precise Point Positioning (PPP) with carrier phase

Professors: Dr. J. Sanz Subirana, Dr. J.M. Juan Zornoza
and Dr. A. Rovira-García

gAGE/UPC research group of Astronomy and Geomatics
BarcelonaTECH, Spain

Contents

Precise Point Positioning (PPP)

The PPP technique allows **centimetre-level** accuracy to be **achieved for static** positioning and **decimetre level, or better, for kinematic positioning, after the best part of one hour.**

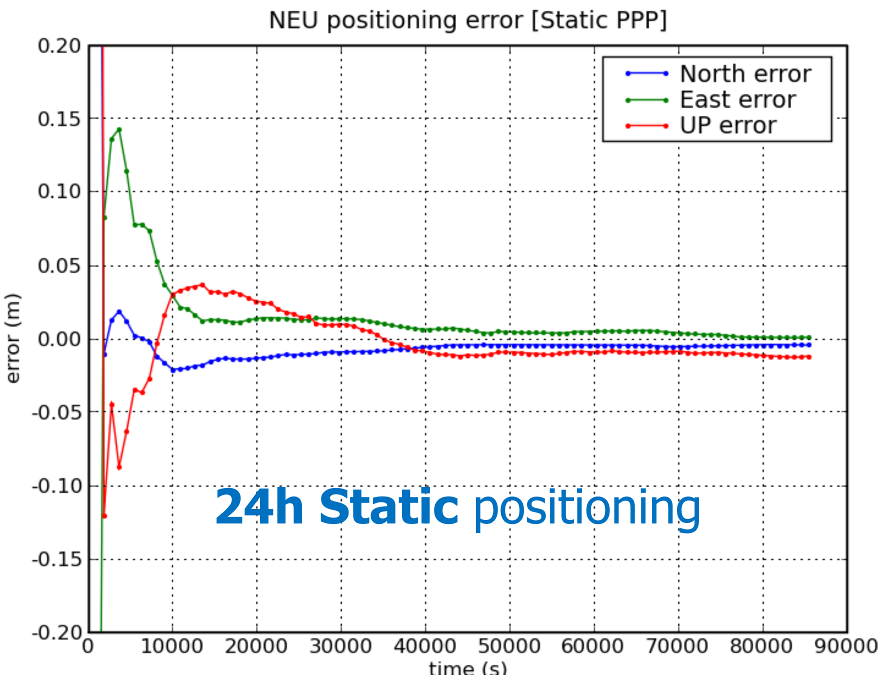

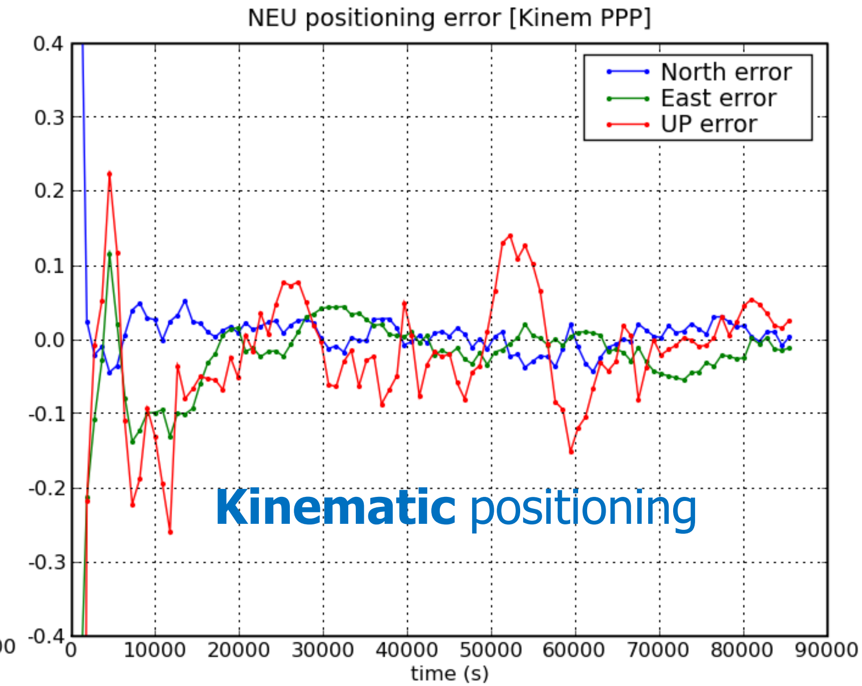

This high accuracy requires the use of code and carrier measurements and an accurate measurement modelling up to centimetre level or better.

Contents

Precise Point Positioning (PPP)

Satellite Orbit and clock accuracies

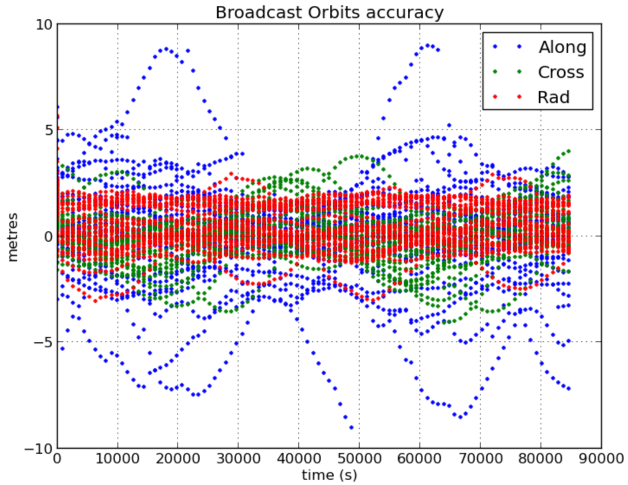

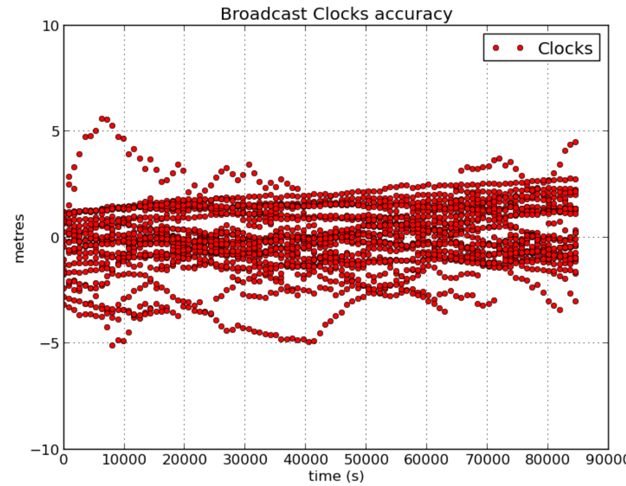

Broadcast:

Few metres of accuracy for broadcast orbits and clocks

Transmitted in the satellite navigation message.

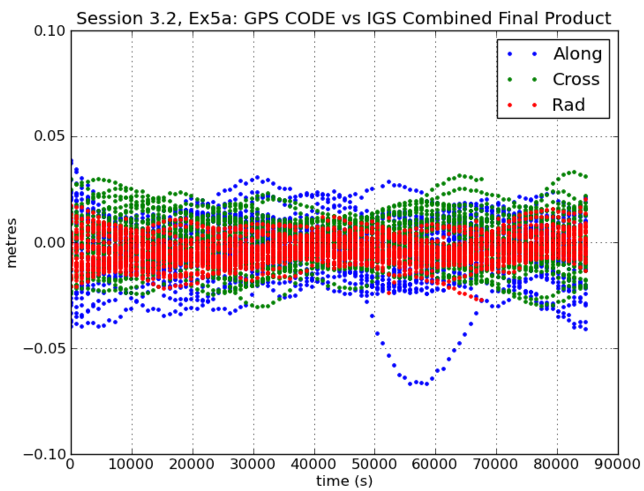

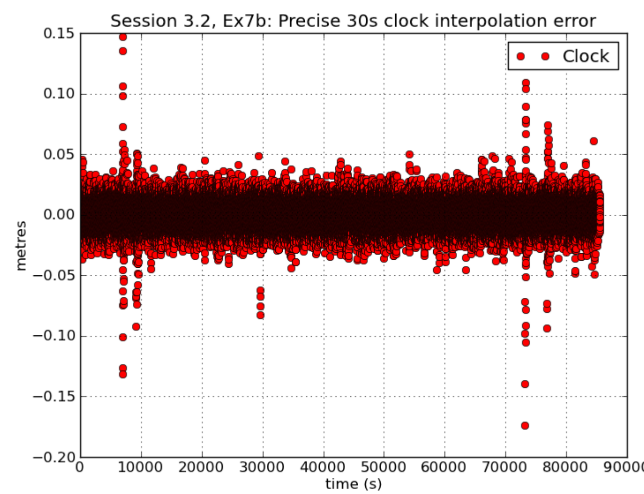

Precise:

Few centimetres of accuracy for precise orbits and clocks

Precise clocks for GPS satellites can be found on the International GNSS Service (IGS) server **http://igscb.jpl.nasa.gov**

IGS Precise orbit and clock products:
RMS accuracy, latency and sampling

Products (delay)	Broadcast (real time)	Ultra-rapid Predicted (real time)	Ultra-rapid Observed (3–9 h)	Rapid (17–41 h)	Final (12–18 d)
Orbit GPS (sampling)	~100 cm (~2 h)	~5 cm (15 min)	~3 cm (15 min)	~2.5cm (15 min)	~ 2.5 cm (15 min)
Glonass (sampling)					~5 cm (15 min)
Clock GPS (sampling)	~5 ns (daily)	~3 ns (15 min)	~150 ps (15 min)	~75 ps (5 min)	~75 ps (30 s)
Glonass (sampling)					~ TBD (15 min)

http://igscb.jpl.nasa.gov/components/prods.html

Computation of satellite coordinates from precise products.

Precise orbits for GPS satellites can be found on the International GNSS Service (IGS) server **http://igscb.jpl.nasa.gov**

Orbits are given by *(x,y,z)* coordinates with a sampling rate of 15 minutes. The satellite coordinates between epochs can be computed by polynomial interpolation. A 10th-order polynomial is enough for a centimetre level of accuracy with 15 min data.

$$
\begin{aligned}
P_n(x) &= \sum_{i=1}^{n} y_i \frac{\prod_{j\neq i}(x-x_j)}{\prod_{j\neq i}(x_i-x_j)} \\
&= y_1 \frac{x-x_2}{x_1-x_2}\cdots\frac{x-x_n}{x_1-x_n}+\cdots \\
&\quad + y_i \frac{x-x_1}{x_i-x_1}\cdots\frac{x-x_{i-1}}{x_i-x_{i-1}}\frac{x-x_{i+1}}{x_i-x_{i+1}}\cdots\frac{x-x_n}{x_i-x_n}+\cdots \\
&\quad + y_n \frac{x-x_1}{x_n-x_1}\cdots\frac{x-x_{n-1}}{x_n-x_{n-1}}
\end{aligned}
$$

IGS orbit and clock products (for PPP):

Discrepancy between the different centres

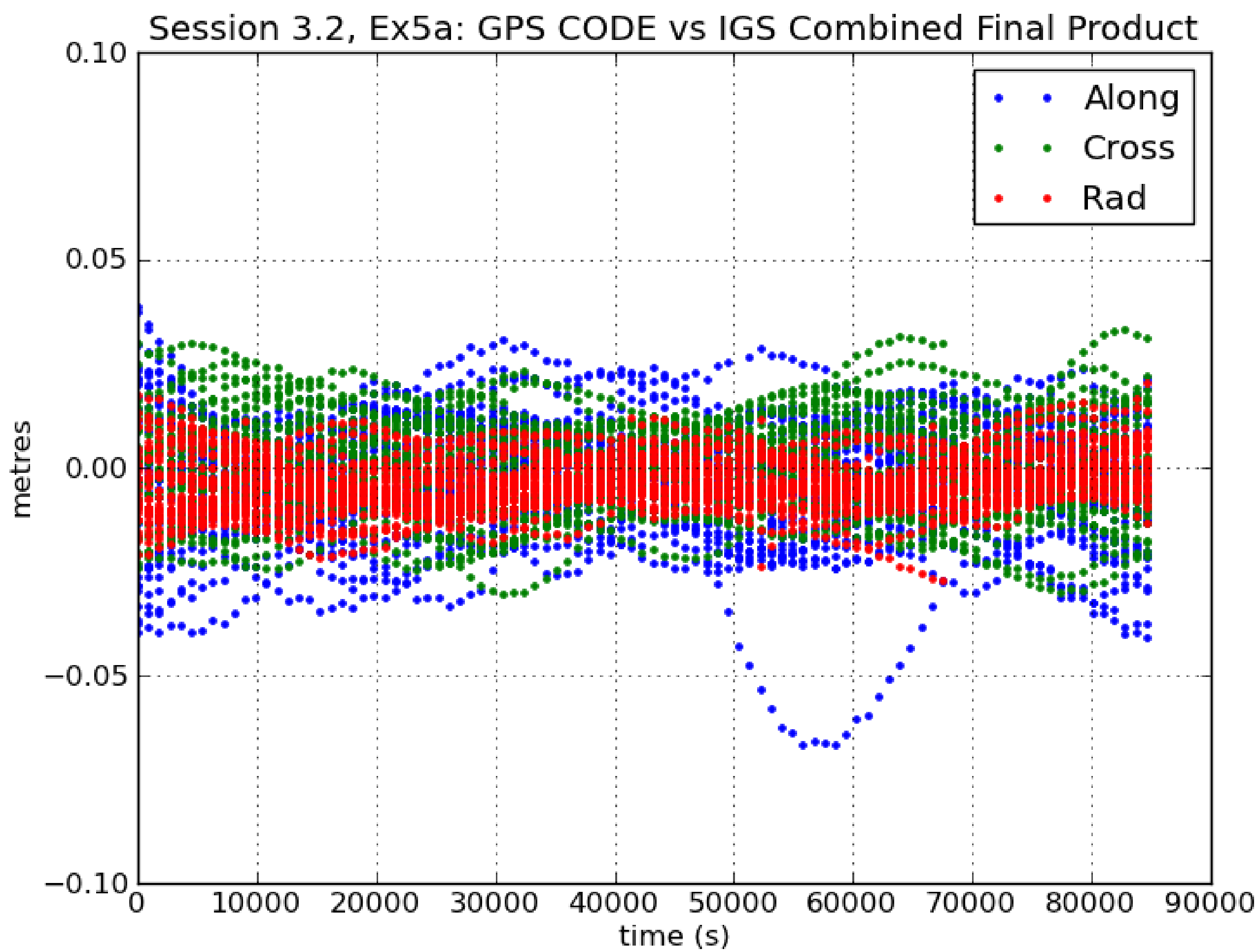

Computation of satellite clocks from precise products

Precise clocks for GPS satellites can be found on the International GNSS Service (IGS) server **http://igscb.jpl.nasa.gov**

IGS is providing precise orbits and clock files with a sampling rate of 15 min, as well as precise clock files with a sample rate of 5 min and 30 sec, in SP3 and CLK formats.

Some centres also provide GPS satellite clocks with a 5 sec sampling rate, like the les obtained from the Crustal Dynamics Data Information System (CDDIS) site.

Stable clocks with a sampling rate of 30 sec or higher can be interpolated with a first-order polynomial to a few centimetres of accuracy. Clocks with a lower sampling rate should not be interpolated, because clocks evolve as random walk processes.

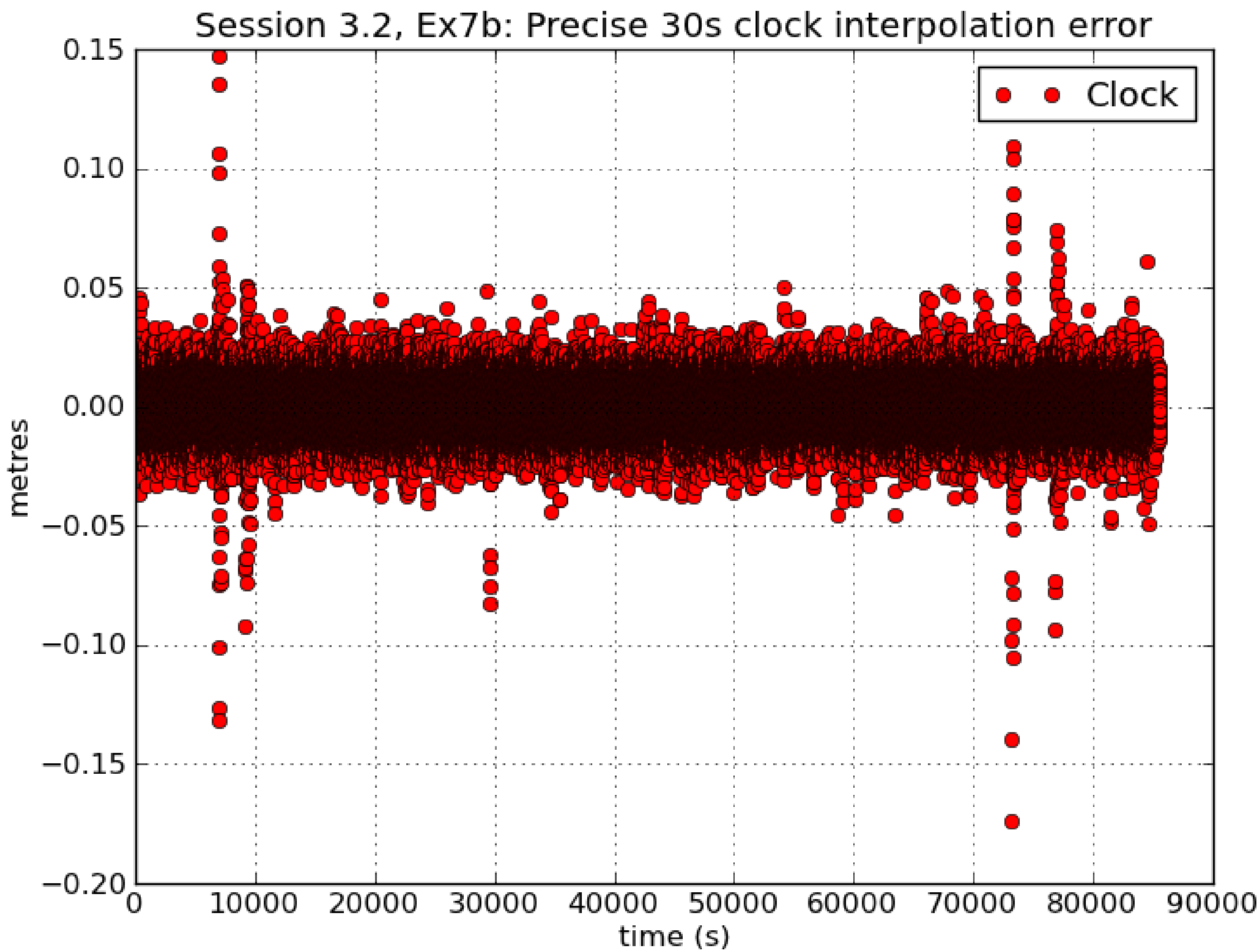
Session 3.2, Ex7b: Precise 30s clock interpolation error
Clock
metres
time (s)
0.15
0.10
0.05
0.00
−0.05
−0.10
−0.15
−0.20
0
10000
20000
30000
40000
50000
60000
70000
80000
90000

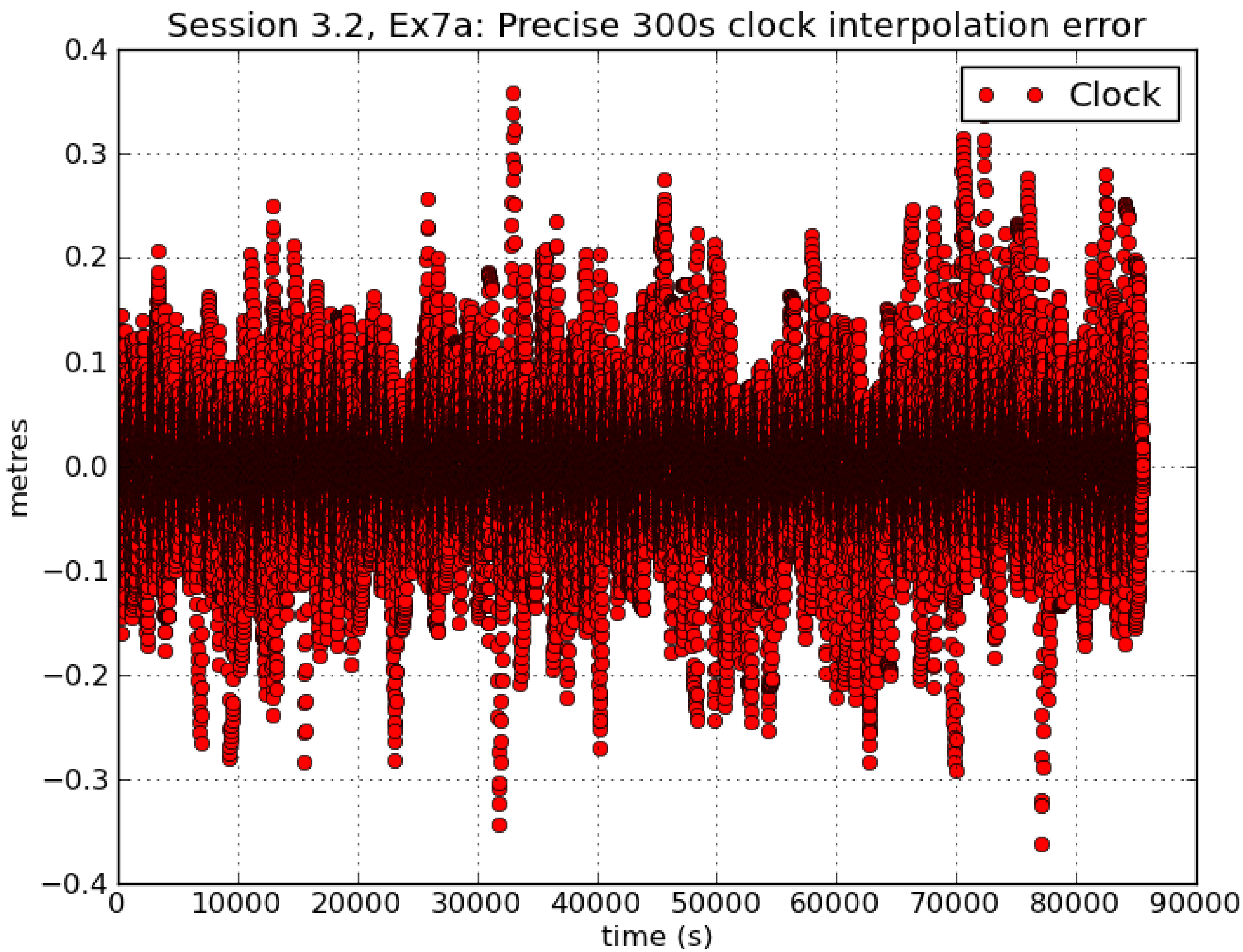
Session 3.2, Ex7a: Precise 300s clock interpolation error
Clock
metres
time (s)
0.4
0.3
0.2
0.1
0.0
−0.1
−0.2
−0.3
−0.4
0
10000
20000
30000
40000
50000
60000
70000
80000
90000

Contents

Precise Point Positioning (PPP)

Measurements: Code and carrier

For high-accuracy positioning, the carrier phase must be used, besides the code pseudorange.

The carrier measurements are very precise, typically at the level of a few millimetres, but contain unknown ambiguities which change every time the receiver locks the signal after a cycle slip.

Nevertheless, such ambiguities can be estimated in the navigation solution, together with the coordinates and other parameters.

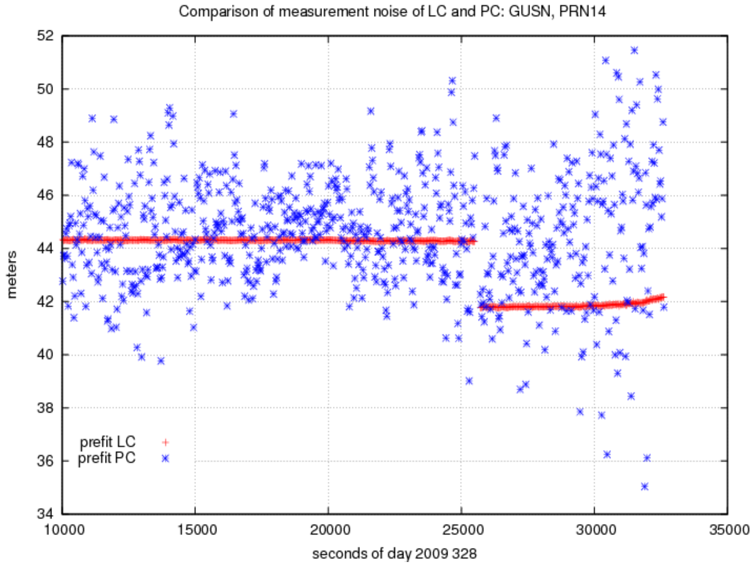

PPP Model components

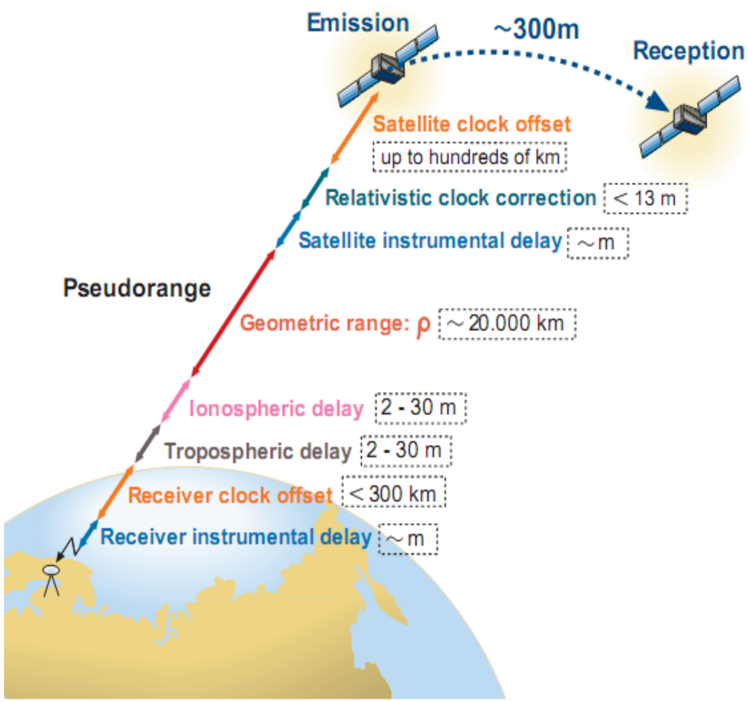

We are going to review first the measurements modelling for the Standard Point Positioning (SPP). A brief summary is given next.

After this summary, we will focus on the additional modelling need for Precise Point Positioning.

Remember that the error component most difficult to model is the ionosphere. But, in the PPP technique the ionosphere error is removed (more than 99.9%) using dual-frequency measurements in the ionosphere-free combination (Lc,Pc). This combination also removes the Differential Code Bias (or TGD).

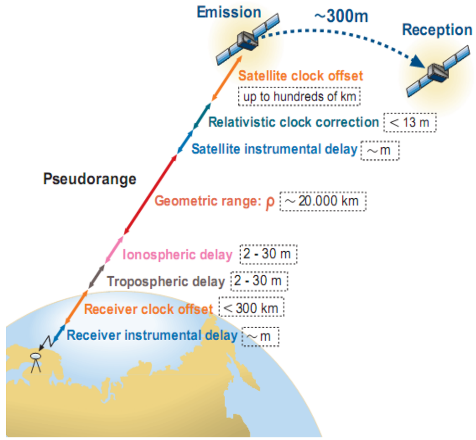

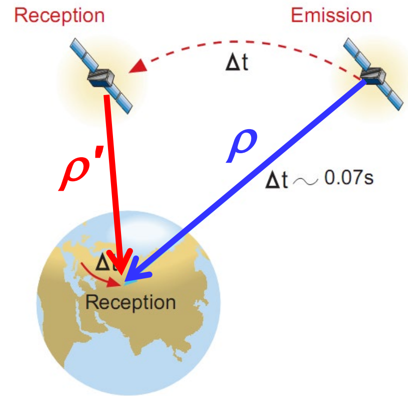

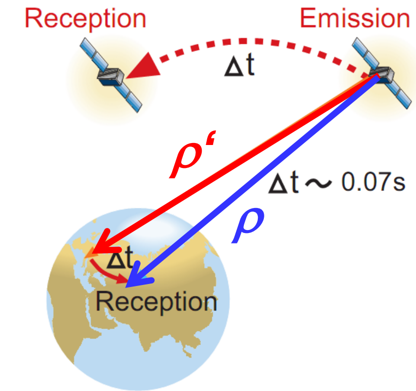

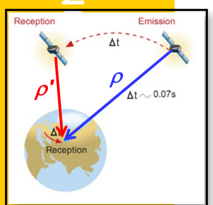

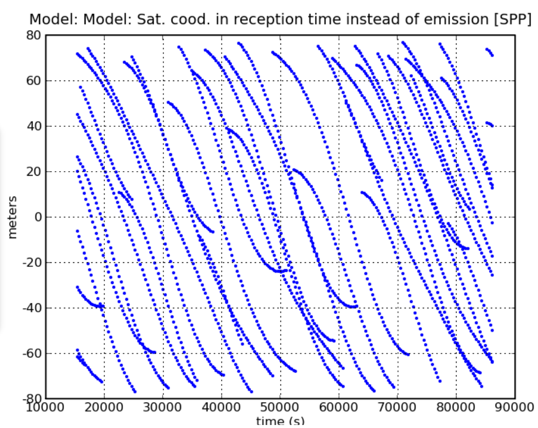

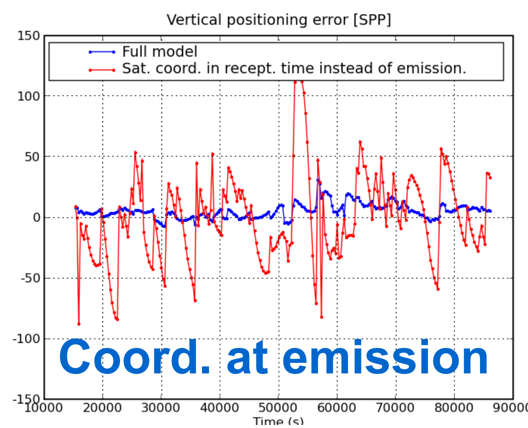

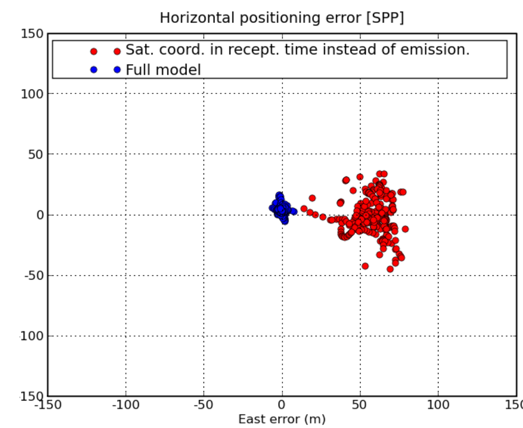

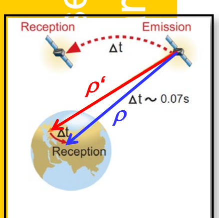

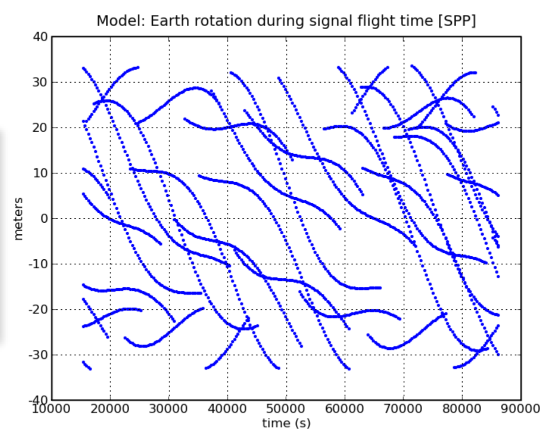

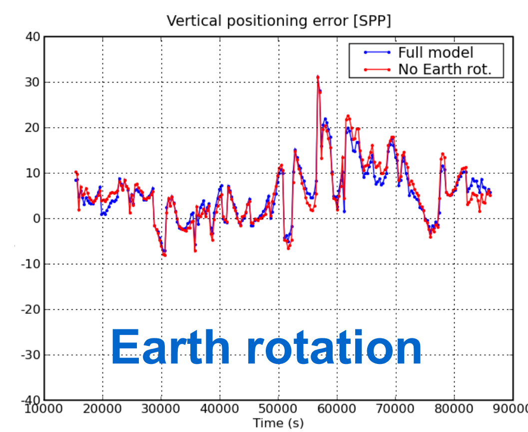

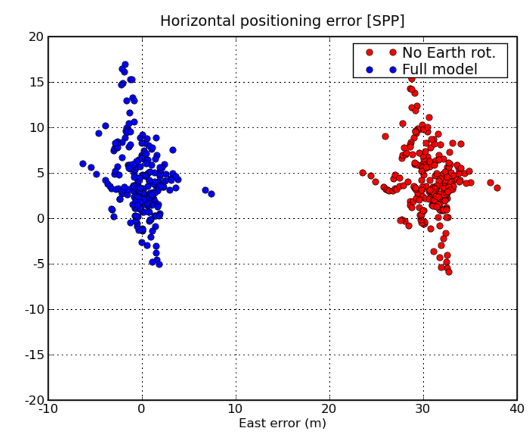

Satellite coordinates computation at signal emission time

gAGE/UPC research group of Astronomy and Geomatics
BarcelonaTECH, Spain

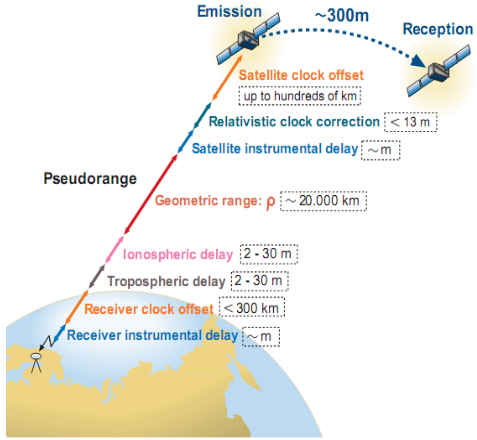

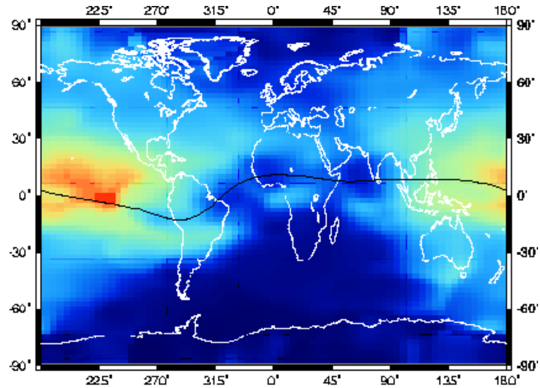

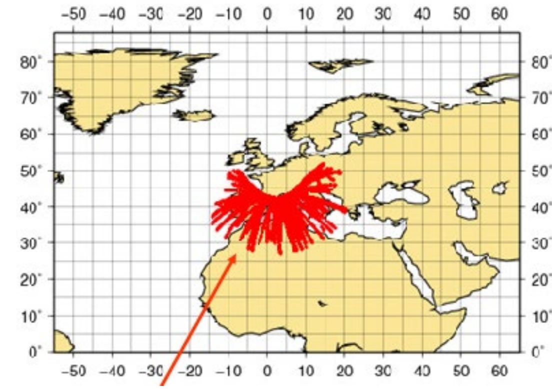

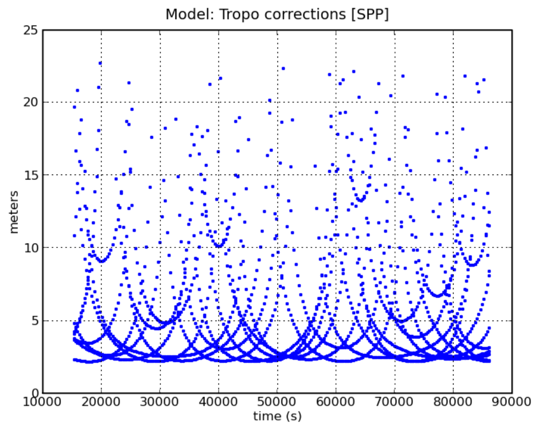

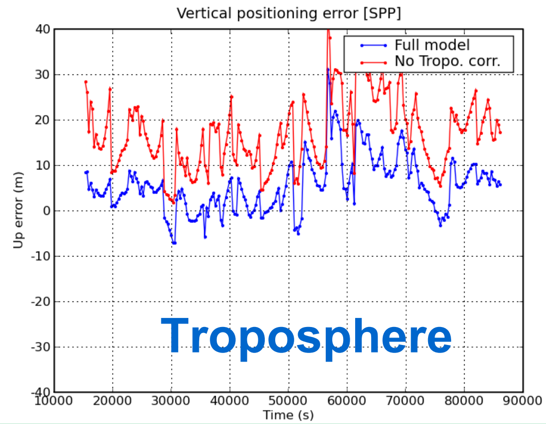

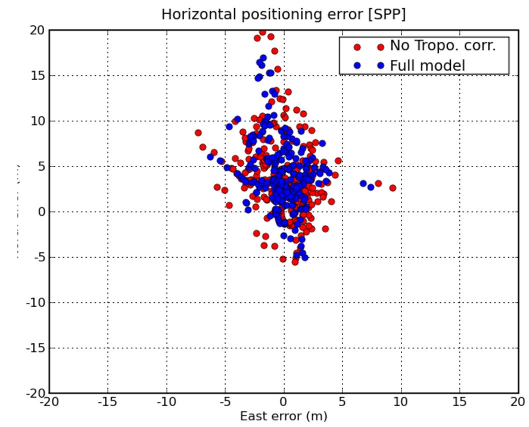

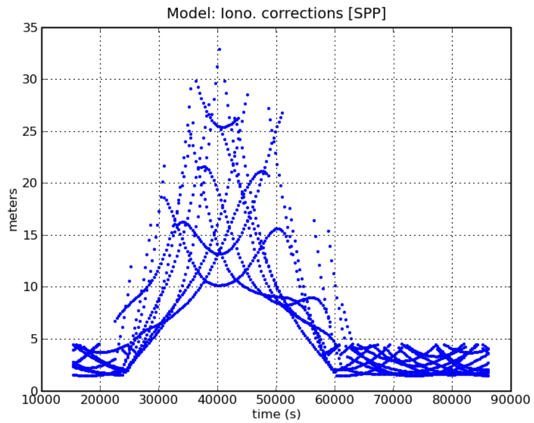

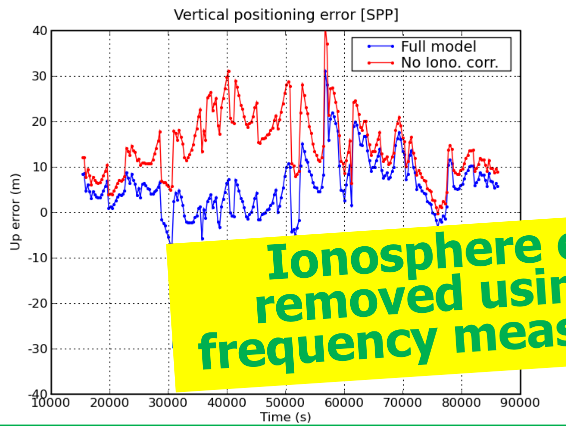

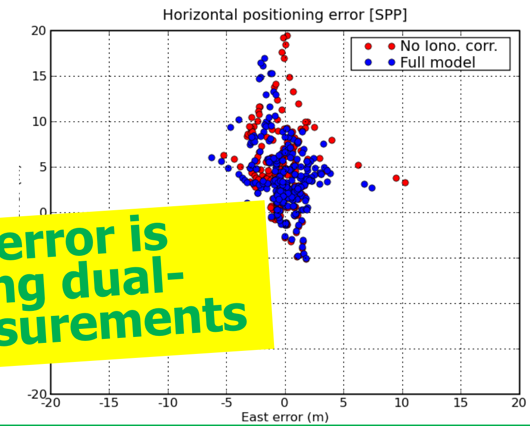

Signal propagation errors on the Atmosphere

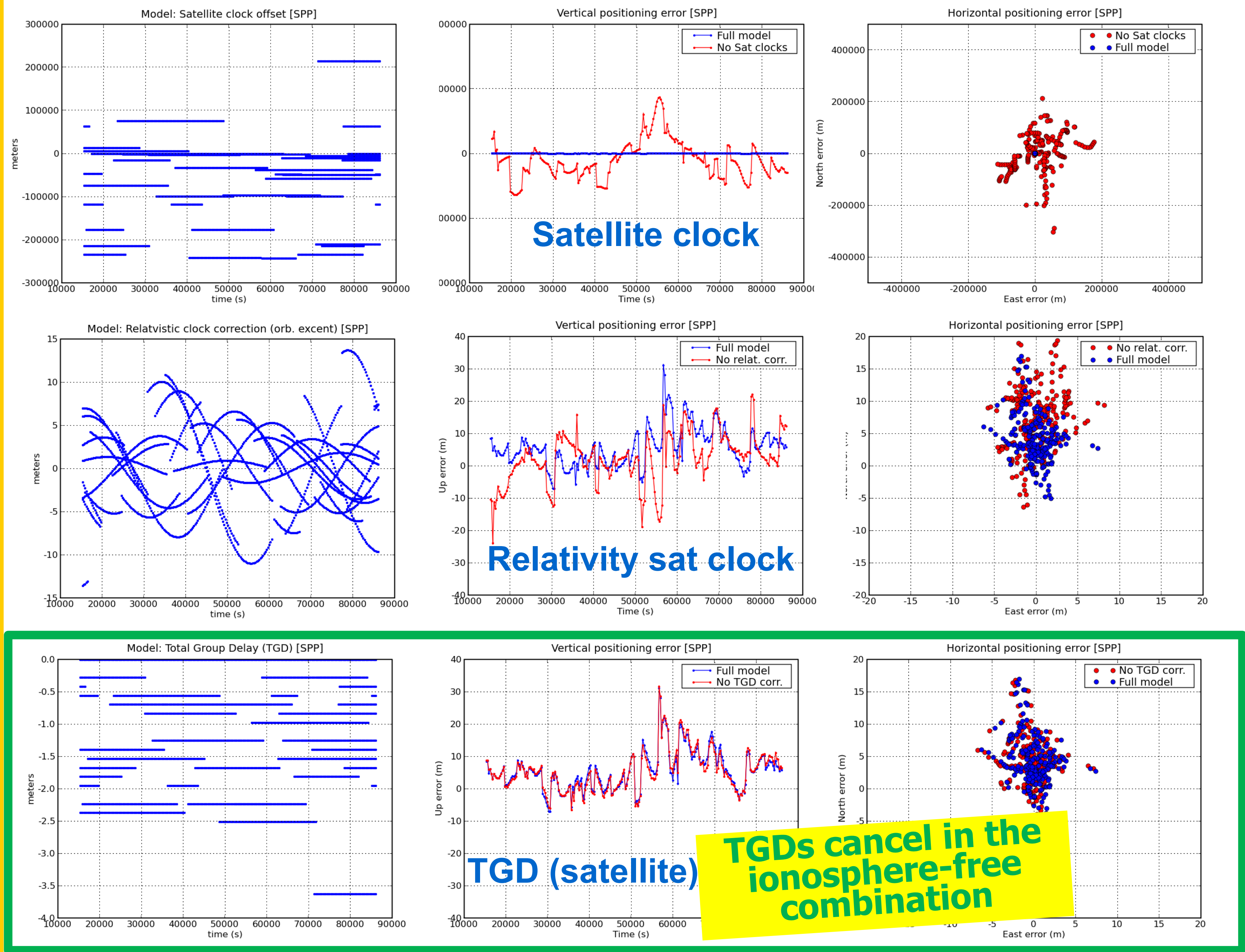

Satellite clocks and Total Group Delay (TGD)

gAGE/UPC research group of Astronomy and Geomatics
BarcelonaTECH, Spain

Additional Modelling for PPP

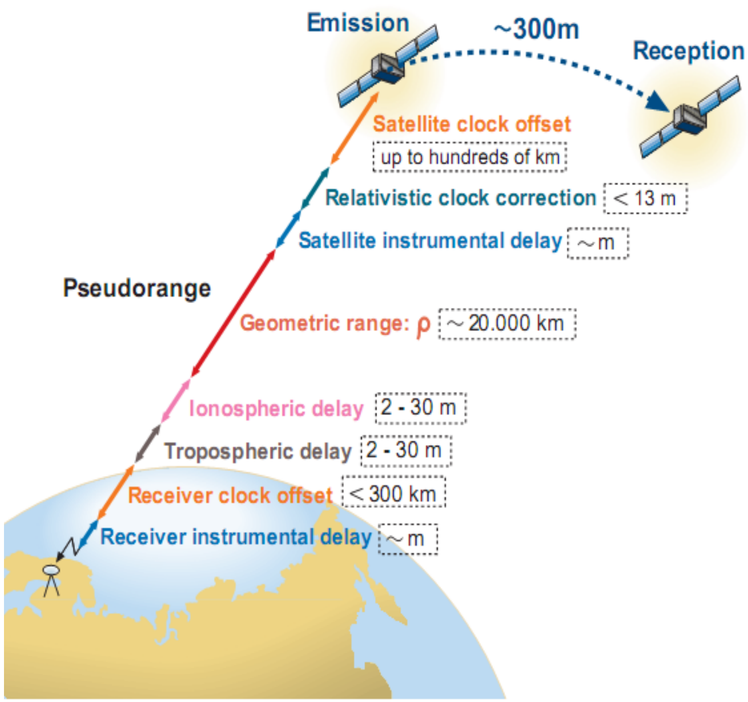

The PPP technique allows centimetre-level of accuracy to be achieved for static positioning and decimetre level, or better, for kinematic navigation.

This high accuracy requires an accurate **modelling "up to the centimetre level or better"** , where all previous model terms must be taken into account (except ionosphere and TGD [*]), **plus some additional terms given next:**

[*] Remember that in the PPP technique the ionosphere error is removed (more than 99.9%) using dual-frequency measurements in the ionosphere-free combination (Lc,Pc). This combination also removes the Differential Code Bias (or TGD).

Additional Modelling for PPP

Satellite Mass Center to Antenna Phase Center

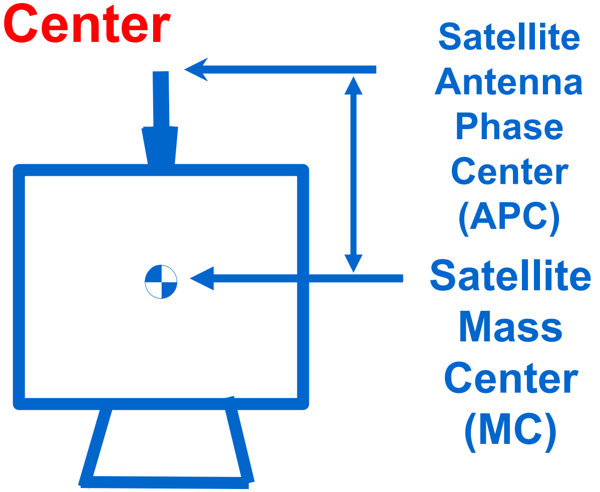

Broadcast orbits are referred to the antenna phase center, but IGS precise orbits are referred to the satellite mass center.

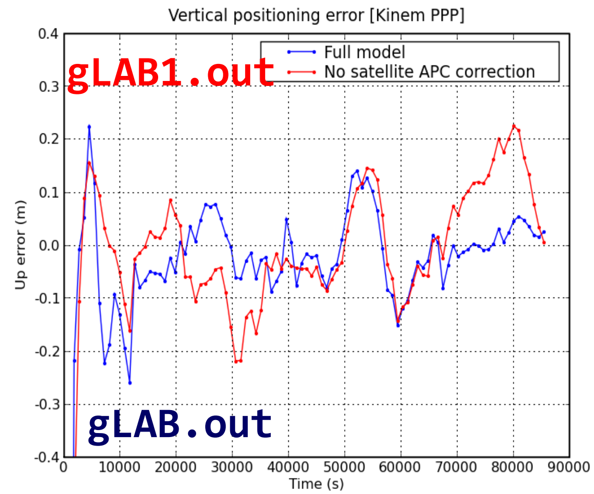

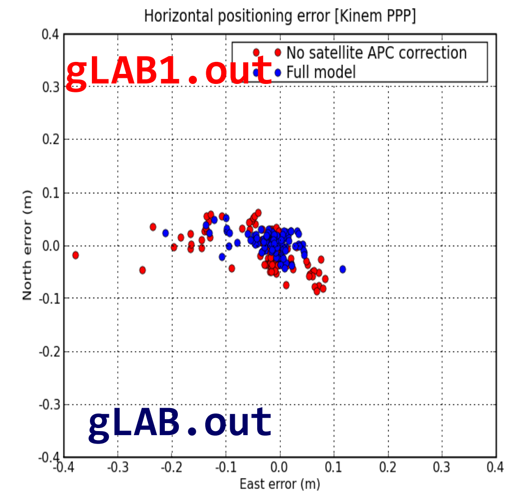

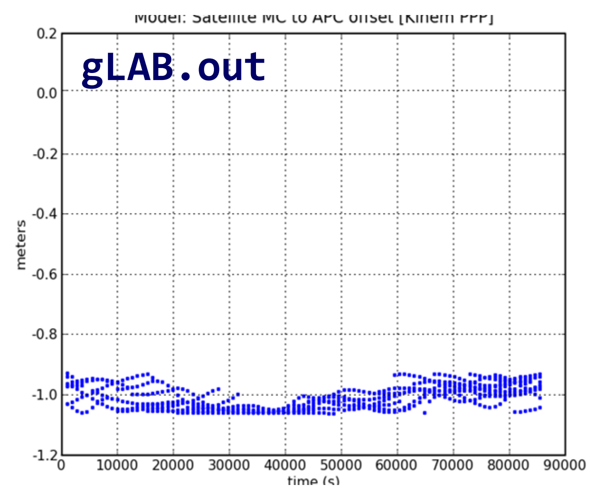

Satellite MC to APC:

The satellite MC to APC eccentricity vector depends on the satellite. The APC values used in the IGS orbits and clocks products are referred to the iono-free combination (LC, PC) . They are given in the IGS ANTEX files (e.g., `igs05.atx`).

Additional Modelling for PPP

Receiver Antenna Phase center (APC)

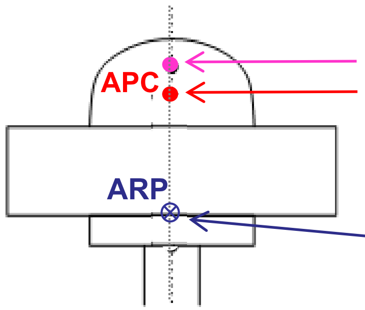

GNSS measurements are referred to the APC. This is not necessarily the geometric center of the antenna, and it depends on the signal frequency and the incoming radio signal direction.

For geodetic positioning a reference tied to the antenna (ARP) or to monument is used

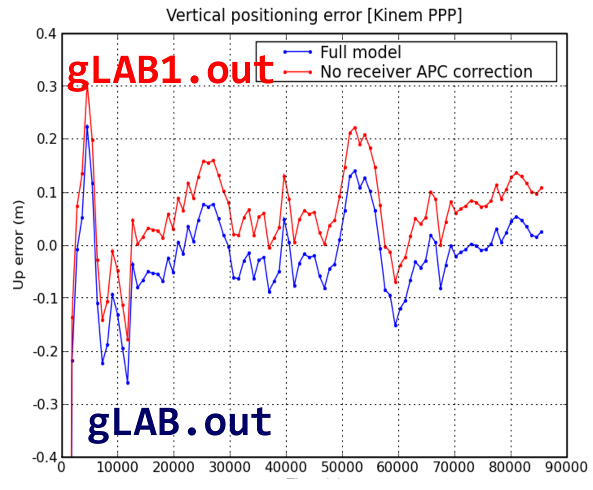

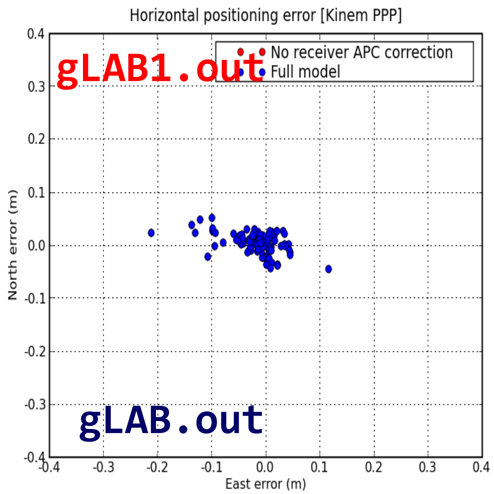

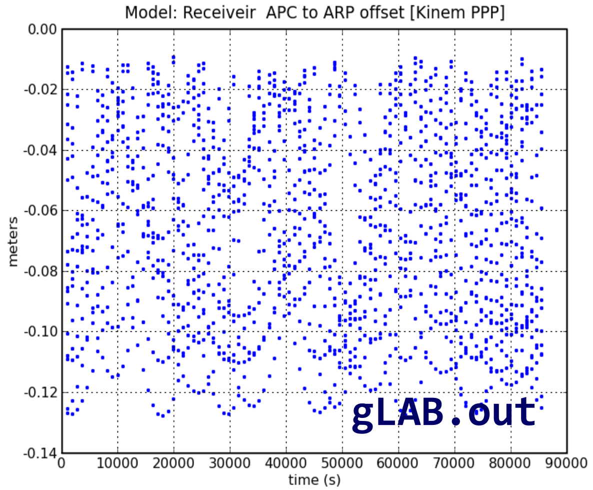

Receiver APC:

The antenna used for this experiment, has the APC position vertically shifted regarding ARP.

Thence, neglecting this correction, an error on the vertical component occurs, but not in the horizontal one.

Additional Modelling for PPP: **APC**

Antenna biases and orientation:

- The satellite and receiver **antenna phase centres (APCs)** can be found in the IGS ANTEX files, after GPS week 1400 (Nov. 2006)
- The **carrier phase wind-up** effect due to the satellite's motion must be taken into account.

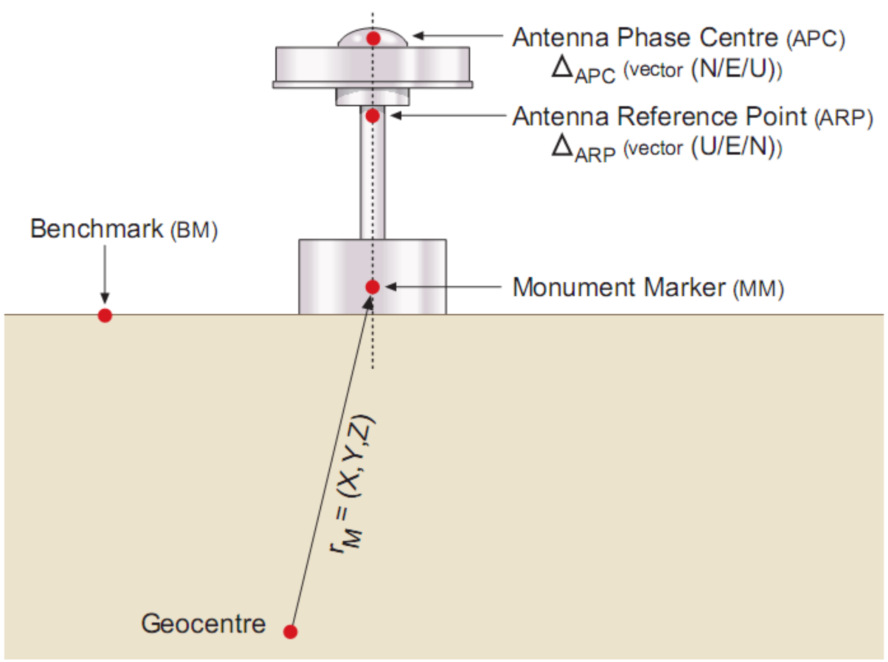

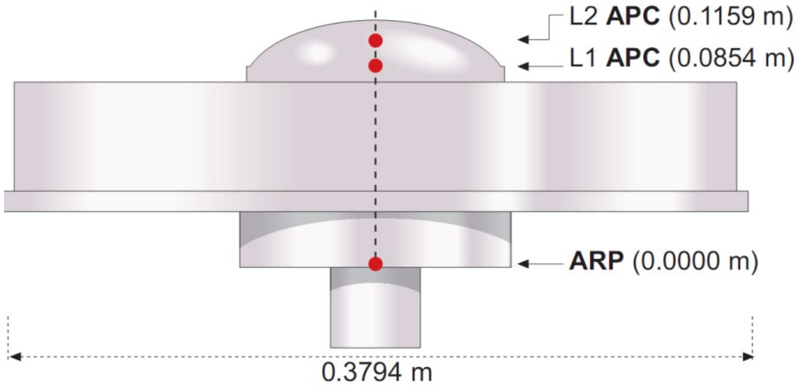

Additional Modelling for PPP

Wind-up affects only carrier phase. It is due to the electromagnetic nature of circularly polarized waves of GNSS signals.

As the satellite moves along its orbital path, it performs a rotation to keep its solar panels pointing to the Sun direction. This rotation causes a carrier variation, and thence, a range measurement variation.

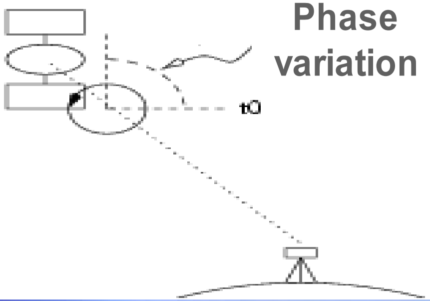

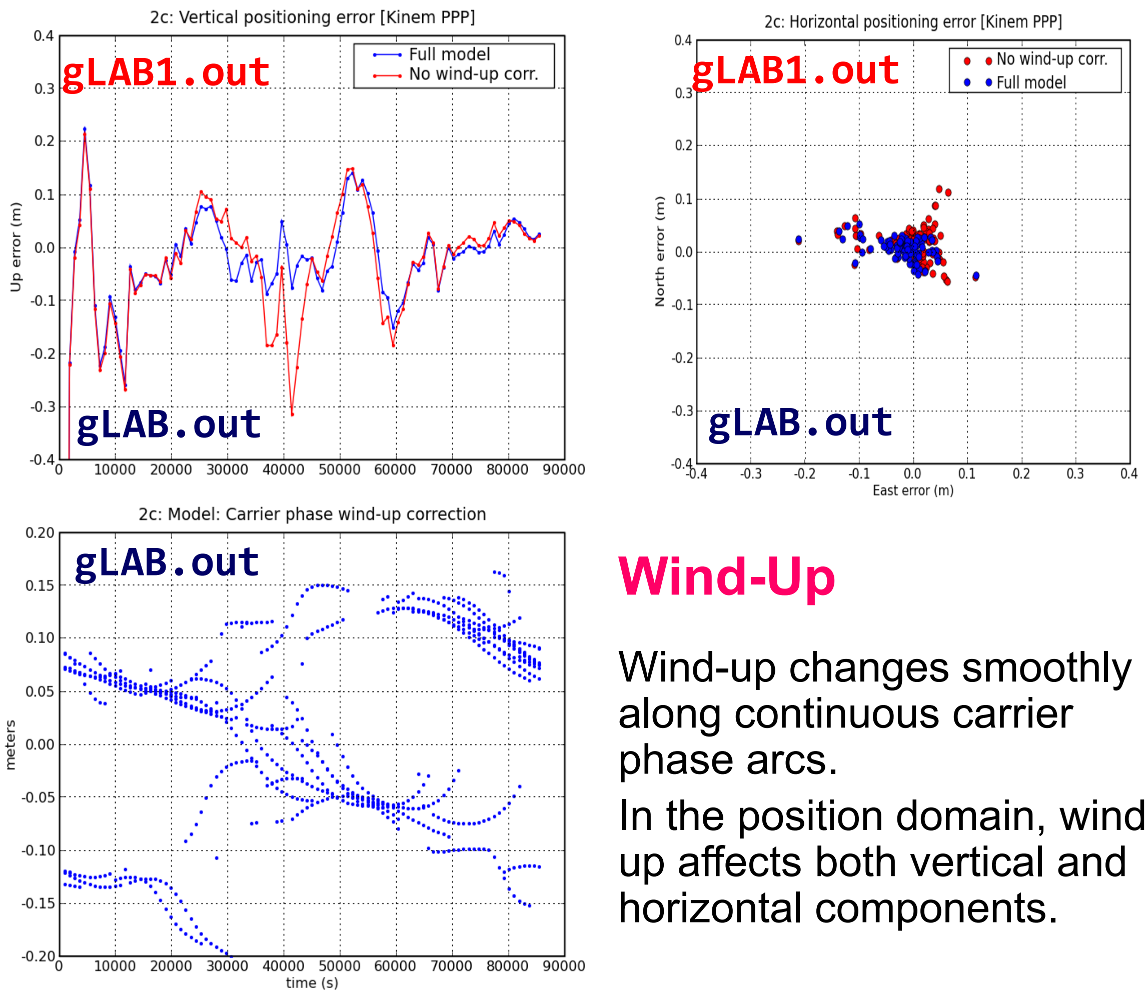

Wind-Up

Wind-up changes smoothly along continuous carrier phase arcs.

In the position domain, wind-up affects both vertical and horizontal components.

Additional Modelling for PPP: **Eclipse condition**

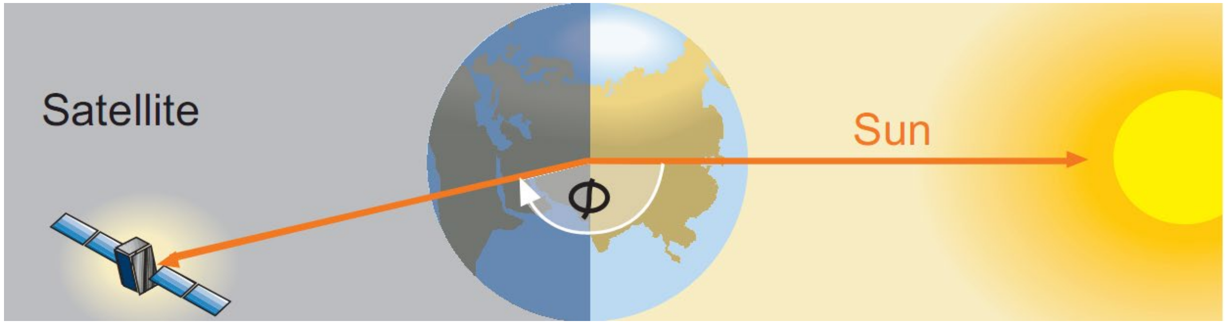

High-accuracy GNSS positioning degrades during the GNSS satellites' eclipse seasons.

- Once the satellite goes into shadow, the radiation pressure vanishes. This effect introduces errors in the satellite dynamics due to the difficulty of properly modelling the solar radiation pressure.
- On the other hand, the satellite's solar sensors lose sight of the Sun and the attitude control (trying to keep the panels facing the Sun).

As a consequence, the orbit during shadow and eclipse periods may be considerably degraded and the removal of satellites under such conditions can improve the high-accuracy positioning results.

Additional Modelling for PPP: **Atmospheric** Effects

- **The ionospheric refraction and TGDs** are **removed** using the ionosphere-free combination of code and carrier measurements (PC, LC).
- **The tropospheric refraction can be modelled by Dry and Wet components** (and different mappings are usually used for both components, e.g. mapping of Niell).

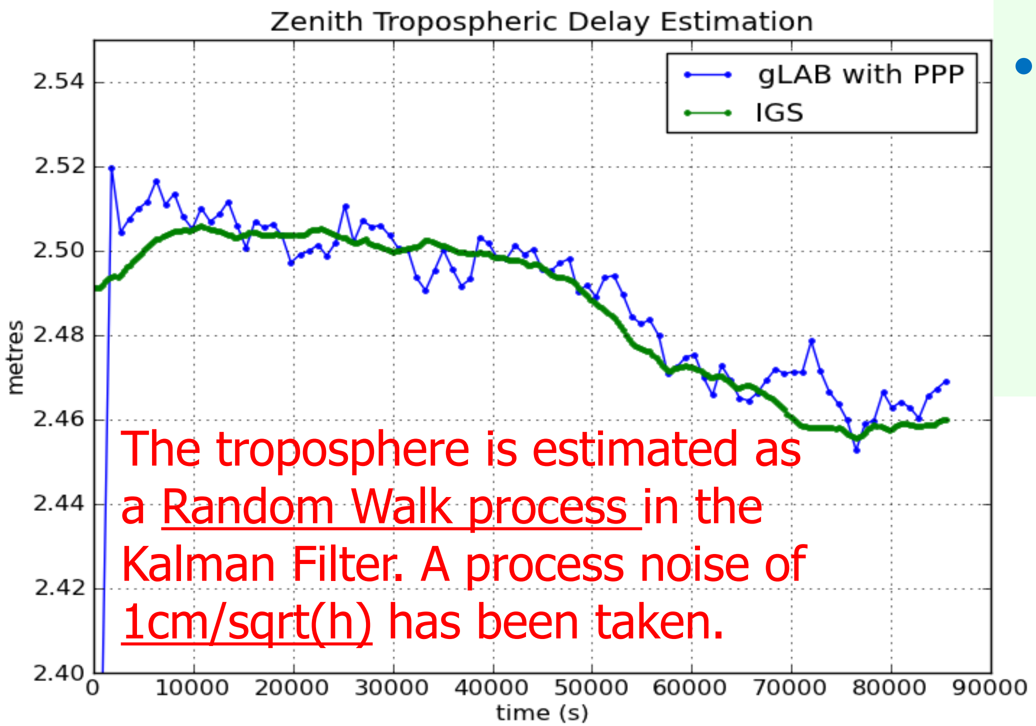

- **A residual tropospheric delay is estimated** (as wet ZTD delay) in the Kalman filter, together with the coordinates, clock and carrier phase ambiguities.

Additional Modelling for PPP: **Earth Deformation**

Earth deformation effects:

- **Solid tides** must be modelled by equations
- **Ocean loading and pole tides** are second-order effects and can be neglected for PPP accuracies at the centimetre level

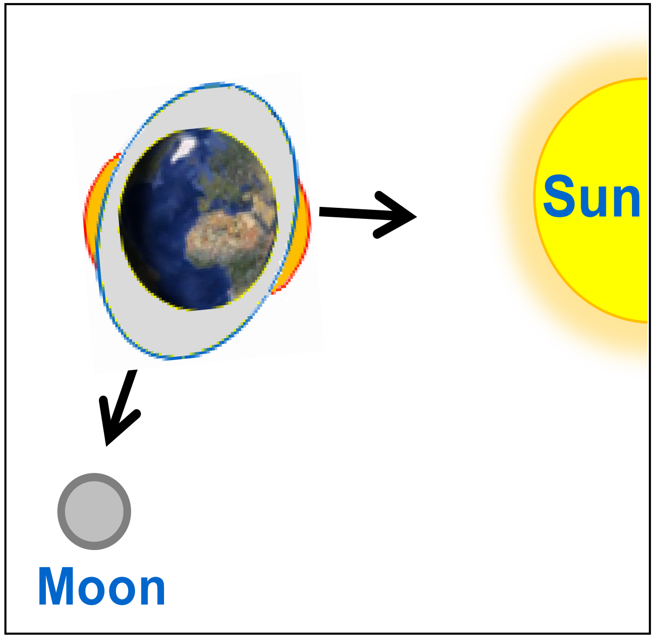

Solid Tides concern the movement of Earth's crust (and thus the variation in the receiver's location coordinates) due to gravitational attractive forces produced by external bodies, mainly the Sun and Moon.

Solid tides produce vertical and horizontal displacements that can be expressed by the spherical harmonics expansion (m, n), characterised by the Love and Shida numbers h_{mn} and l_{mn}.

Additional Modelling for PPP

Solid Tides

It comprises the Earth's crust movement (and thence receiver coordinates variations) due to the gravitational attraction forces produced by external bodies, mainly the Sun and the Moon.

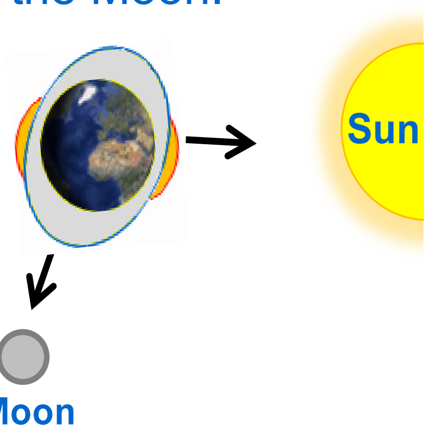

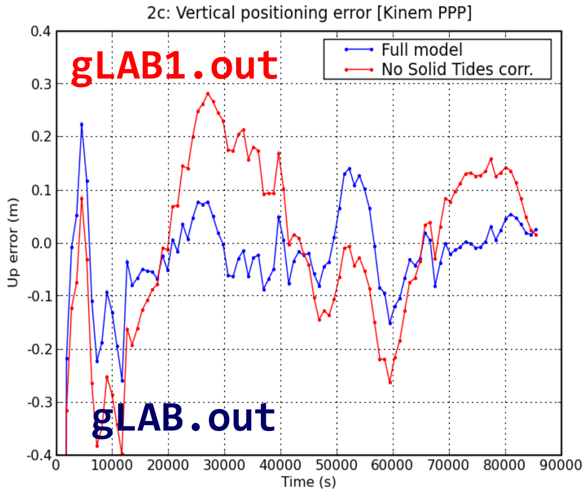

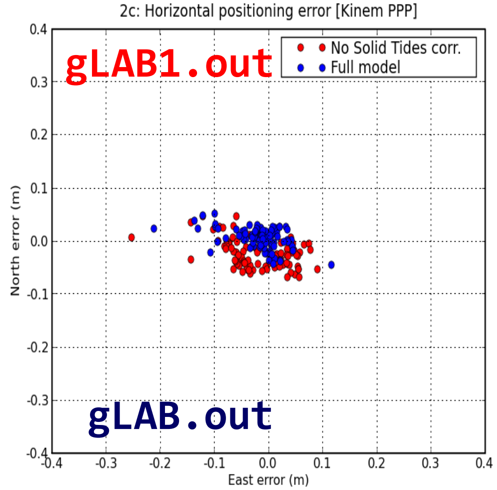

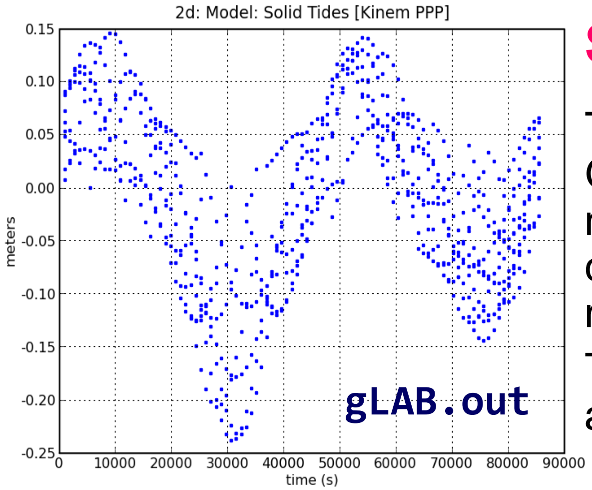

Solid Tides:

These effects do not affect the GNSS signals, but if they were not considered, the station coordinates would oscillate with relation to a mean value.

They produce vertical (mainly) and horizontal displacements.

Contents

Precise Point Positioning (PPP)

Linear observation model for PPP

It is based code and carrier measurements in the ionosphere-free combination (Pc, Lc), which are modelled as follows:

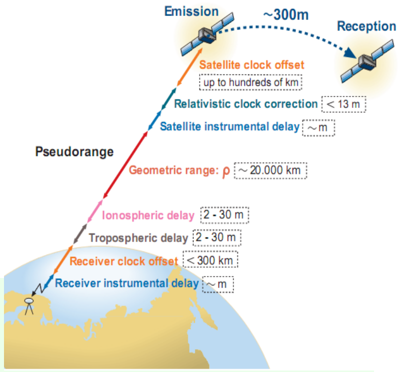

$$P_{C\,rec}^{\,sat} = \rho_{rec}^{sat} + c\cdot(dt_{rec} - dt^{sat}) + Trop_{rec}^{sat} + \mathcal{M}_{Pc} + \varepsilon_{P_C}$$

$$L_{C\,rec}^{\,sat} = \rho_{rec}^{sat} + c\cdot(dt_{rec} - dt^{sat}) + Trop_{rec}^{sat} + \lambda_N \omega_{rec}^{sat} + B_{C\,rec}^{\,sat} + m_{L_C} + \varepsilon_{L_C}$$

where

$$P_C = \frac{f_1^2 P_1 - f_2^2 P_2}{f_1^2 - f_2^2}; \quad L_C = \frac{f_1^2 L_1 - f_2^2 L_2}{f_1^2 - f_2^2}$$

$$B_C = \lambda_N \left(B_1 + \frac{\lambda_W}{\lambda_2} B_W \right)$$

$$B_W = B_1 - B_2$$

λ_N= 10.7 cm, λ_W=86.2cm

Ionosphere is removed

Remark, ρ is referred to the Antenna Phase Centres (APC) of satellite and receiver antennas in the ionosphere free combination.

Linear model: For each satellite in view

$$P_{C\,rec}^{\,sat} = \rho_{rec}^{sat} + c\cdot(dt_{rec} - dt^{sat}) + Trop + \varepsilon$$

Linearising $\boldsymbol{\rho}$ around an 'a priori' receiver position $(x_{rec,0}, y_{rec,0}, z_{rec,0})$

$$= \boxed{\rho_{rec,o}^{sat} + \frac{x_{rec,o} - x^{sat}}{\rho_{rec,o}^{sat}}\Delta x_{rec} + \frac{y_{rec,o} - y^{sat}}{\rho_{rec,o}^{sat}}\Delta y_{rec} + \frac{z_{rec,o} - z^{sat}}{\rho_{rec,o}^{sat}}\Delta z_{rec}} + c\left(dt_{rec} - dt^{sat}\right) + Trop$$

where:

$$\Delta x_{rec} = x_{rec} - x_{rec,o} \quad ; \quad \Delta y_{rec} = y_{rec} - y_{rec,o} \quad ; \quad \Delta z_{rec} = z_{rec} - z_{rec,o}$$

and taking: $Trop_{rec}^{sat} = Trop_{0\,rec}^{\;sat} + M_{wet,rec}^{\,sat}\,\Delta Tr_{Z,wet}$

Prefit-residuals (Prefit)

$$\boxed{P_{C\,rec}^{\,sat} - \left(\rho_{rec,o}^{sat} + c\,dt^{sat} - Trop_{0rec}^{\;sat}\right)} = \frac{x_{rec,o} - x^{sat}}{\rho_{rec,o}^{sat}}\Delta x_{rec} + \frac{y_{rec,o} - y^{sat}}{\rho_{rec,o}^{sat}}\Delta y_{rec} + \frac{z_{rec,o} - z^{sat}}{\rho_{rec,o}^{sat}}\Delta z_{rec} + c\,dt_{rec} + M_{wet}^{\,sat}\,\Delta Tr_{Z,wet}$$

measurement

computed

unknown

The same for carrier, but adding the ambiguity as an unknown

Remark

$$P_{C\,rec}^{\;sat} = \rho_{rec}^{sat} + c\cdot(dt_{rec} - dt^{sat}) + Trop + \varepsilon$$

Linearising $\boldsymbol{\rho}$ around an 'a priori' receiver position $(x_{rec,0}, y_{rec,0}, z_{rec,0})$

$$= \rho_{rec,o}^{sat} + \frac{x_{rec,o} - x^{sat}}{\rho_{rec,o}^{sat}}\Delta x_{rec} + \frac{y_{rec,o} - y^{sat}}{\rho_{rec,o}^{sat}}\Delta y_{rec} + \frac{z_{rec,o} - z^{sat}}{\rho_{rec,o}^{sat}}\Delta z_{rec} + c\left(dt_{rec} - dt^{sat}\right) + Trop$$

Of course, receiver coordinates $(x_{rec}, y_{rec}, z_{rec})$ are not known (they are the target of this problem). But, we can always assume that an "approximate position $(x_{0,rec}, y_{0,rec}, z_{0,rec})$ is known".

Thence, the navigation problem will consist on:

1.- To start from an approximate value for receiver position $(x_{0,rec}, y_{0,rec}, z_{0,rec})$ e.g. the Earth's centre) to linearise the equations

2.- With the pseudorange measurements and the navigation equations, compute the correction $(\Delta x_{rec}, \Delta y_{rec}, \Delta z_{rec})$ to have improved estimates:

$$(x_{rec}, y_{rec}, z_{rec}) = (x_{0,rec}, y_{0,rec}, z_{0,rec}) + (\Delta x_{rec}, \Delta y_{rec}, \Delta z_{rec})$$

3.- Linearise the equations again, about the new improved estimates, and iterate until the change in the solution estimates is small enough.

gAGE

Linear model: For each satellite in view

$$\boxed{P_{C\,rec}^{\,sat} = \rho_{rec}^{sat} + c\cdot(dt_{rec} - dt^{sat}) + Trop + \varepsilon}$$

Linearising ρ around an 'a priori' receiver position $(x_{rec,0}, y_{rec,0}, z_{rec,0})$

$$= \boxed{\rho_{rec,o}^{sat} + \frac{x_{rec,o} - x^{sat}}{\rho_{rec,o}^{sat}}\Delta x_{rec} + \frac{y_{rec,o} - y^{sat}}{\rho_{rec,o}^{sat}}\Delta y_{rec} + \frac{z_{rec,o} - z^{sat}}{\rho_{rec,o}^{sat}}\Delta z_{rec}} + c\left(dt_{rec} - dt^{sat}\right) + Trop$$

where:

$$\Delta x_{rec} = x_{rec} - x_{rec,o} \quad ; \quad \Delta y_{rec} = y_{rec} - y_{rec,o} \quad ; \quad \Delta z_{rec} = z_{rec} - z_{rec,o}$$

and taking: $Trop_{rec}^{sat} = Trop_{0\,rec}^{\,sat} + M_{wet,rec}^{\,sat}\,\Delta Tr_{Z,wet}$

Prefit-residuals (Prefit)

$$\boxed{P_{C\,rec}^{\,sat} - \left(\rho_{rec,o}^{sat} + c\,dt^{sat} - Trop_{0rec}^{\,sat}\right)} = \frac{x_{rec,o} - x^{sat}}{\rho_{rec,o}^{sat}}\Delta x_{rec} + \frac{y_{rec,o} - y^{sat}}{\rho_{rec,o}^{sat}}\Delta y_{rec} + \frac{z_{rec,o} - z^{sat}}{\rho_{rec,o}^{sat}}\Delta z_{rec} + c\,dt_{rec} + M_{wet}^{\,sat}\,\Delta Tr_{Z,wet}$$

measurement

computed

unknown

The same for carrier, but adding the ambiguity as an unknown

Linear model: For each satellite in view

$$P_{C\,rec}^{\;sat} = \rho_{rec}^{sat} + c\cdot(dt_{rec} - dt^{sat}) + Trop + \varepsilon$$

Linearising ρ around an 'a priori' receiver position $(x_{rec,0}, y_{rec,0}, z_{rec,0})$

$$= \rho_{rec,o}^{sat} + \frac{x_{rec,o}-x^{sat}}{\rho_{rec,o}^{sat}}\Delta x_{rec} + \frac{y_{rec,o}-y^{sat}}{\rho_{rec,o}^{sat}}\Delta y_{rec} + \frac{z_{rec,o}-z^{sat}}{\rho_{rec,o}^{sat}}\Delta z_{rec} + c\left(dt_{rec} - dt^{sat}\right) + Trop$$

where:

$$\Delta x_{rec} = x_{rec} - x_{rec,o} \quad ; \quad \Delta y_{rec} = y_{rec} - y_{rec,o} \quad ; \quad \Delta z_{rec} = z_{rec} - z_{rec,o}$$

and taking: $Trop_{rec}^{sat} = Trop_{0\,rec}^{\;sat} + M_{wet,rec}^{sat}\,\Delta Tr_{Z,wet}$

Prefit-residuals (Prefit)

$$P_{C\,rec}^{\;sat} - \rho_{rec,o}^{sat} + c\,dt^{sat} - Trop_{0rec}^{\;sat} = \frac{x_{rec,o}-x^{sat}}{\rho_{rec,o}^{sat}}\Delta x_{rec} + \frac{y_{rec,o}-y^{sat}}{\rho_{rec,o}^{sat}}\Delta y_{rec} + \frac{z_{rec,o}-z^{sat}}{\rho_{rec,o}^{sat}}\Delta z_{rec} + c\,dt_{rec} + M_{wet}^{sat}\,\Delta Tr_{Z,wet}$$

$$L_{C\,rec}^{\;sat} - \rho_{rec,o}^{sat} + c\,dt^{sat} - Trop_{0rec}^{\;sat} - \lambda_N \omega^{sat} = \frac{x_{rec,o}-x^{sat}}{\rho_{rec,o}^{sat}}\Delta x_{rec} + \frac{y_{rec,o}-y^{sat}}{\rho_{rec,o}^{sat}}\Delta y_{rec} + \frac{z_{rec,o}-z^{sat}}{\rho_{rec,o}^{sat}}\Delta z_{rec} + c\,dt_{rec} + M_{wet}^{sat}\,\Delta Tr_{Z,wet} + B_C^{sat}$$

unknowns

gAGE

Following the same procedure as with the code based positioning (SPP), the linear observation model $\mathbf{y} = \mathbf{G}\,\mathbf{x}$ for the code and carrier measurements can be written as follows:

$$\mathbf{y} = \mathbf{G}\,\mathbf{x}$$

$$\begin{bmatrix} Prefit(Pc)^1 \\ Prefit(Lc)^1 \\ \cdots\cdots \\ Prefit(Pc)^n \\ Prefit(Lc)^n \end{bmatrix} = \begin{bmatrix} \frac{x_{o,rec}-x^1}{\rho^1_{0,rec}} & \frac{y_{o,rec}-y^1}{\rho^1_{0,rec}} & \frac{z_{o,rec}-z^1}{\rho^1_{0,rec}} & 1 & M^1_{wet} & 0 & \cdots & \cdots & 0 \\ \frac{x_{o,rec}-x^1}{\rho^1_{0,rec}} & \frac{y_{o,rec}-y^1}{\rho^1_{0,rec}} & \frac{z_{o,rec}-z^1}{\rho^1_{0,rec}} & 1 & M^1_{wet} & 1 & \cdots & \cdots & 0 \\ \cdots & \cdots & \cdots & \cdots & \cdots & \cdots & \cdots & \cdots & \cdots \\ \frac{x_{o,rec}-x^n}{\rho^n_{0,rec}} & \frac{y_{o,rec}-y^n}{\rho^n_{0,rec}} & \frac{z_{o,rec}-z^n}{\rho^n_{0,rec}} & 1 & M^n_{wet} & 0 & \cdots & \cdots & 0 \\ \frac{x_{o,rec}-x^n}{\rho^n_{0,rec}} & \frac{y_{o,rec}-y^n}{\rho^n_{0,rec}} & \frac{z_{o,rec}-z^n}{\rho^n_{0,rec}} & 1 & M^n_{wet} & 0 & \cdots & \cdots & 1 \end{bmatrix} \begin{bmatrix} \Delta x_{rec} \\ \Delta y_{rec} \\ \Delta z_{rec} \\ cdt_{rec} \\ \Delta Tr_{Z,wet} \\ B_C^{\,1} \\ \cdots \\ B_C^{\,n} \end{bmatrix}$$

$$Prefit(P_C)^k = P_C^{\,k} - \rho_0^k + cdt^k - Trop_0^k$$

$$Prefit(L_C)^k = L_C^{\,k} - \rho_0^k + cdt^k - Trop_0^k - \lambda_N \omega^k$$

Carrier ambiguities

Contents

Precise Point Positioning (PPP)

Parameter estimation PPP: Floating Ambiguities

The linear observation model $\mathbf{y} = \mathbf{G}\,\mathbf{x}$ can be solved using the **Kalman filter**. The next stochastic model can be used

- **Carrier phase ambiguities** (B_C) are taken as 'constant' along continuous phase arcs, and as `white noise´ when a cycle slip happens ($\sigma = 10^4\ m$ can be taken, for instance) ➔ **FLOATED AMB.**
- **Wet tropospheric delay** ($Tr_{z;wet}$) is taken as a random walk process (with $d\sigma^2/dt = 1\ cm^2/h$, for instance).
- **Receiver clock** (cdt) is taken as a white-noise process (with $\sigma = 3.10^5\ m$, i.e. $1\ ms$ for instance).
- **Receiver coordinates** ($\Delta x, \Delta y, \Delta z$)
  - For **static positioning** the coordinates are taken as constants.
  - For **kinematic positioning** the coordinates are taken as white noise or a random walk process.

Comment: Floating Ambiguities

This solution procedure is called **floating ambiguities**. 'Floating' in the sense that the ambiguities are estimated by the filter 'as real numbers'.

The bias estimations $\hat{B}_C$ will converge to a solution after a transition time that depends on the observation geometry, model quality and data noise.

In general, one must expect errors at the decimetre level, or better, in pure kinematic positioning (after the best part of one hour) and at the centimetre level in static PPP over 24h data.

See exercises in the laboratory session.

Contents

Carrier Ambiguity Fixing concept

In the previous formulation, the ambiguities have been estimated as real numbers in the Kalman filter, without exploiting its integer nature.

That is, the ambiguities in L_1, L_2 or L_W signals are an integer number (N) of its associated wavelength (λ) plus a fractional part associated to the satellite and to the receiver.

$$B_{1,rec}^{sat} = \lambda_1 N_{1,rec}^{sat} + b_{1,rec} + b_1^{sat}$$

$$B_{2,rec}^{sat} = \lambda_2 N_{2,rec}^{sat} + b_{2,rec} + b_2^{sat}$$

$$N_W = N_1 - N_2$$

$$\boxed{B_C = \lambda_N \left(N_1 + \frac{\lambda_w}{\lambda_2} N_W \right) + b_{C,rec} + b_C^{sat}}$$

Bc is not an integer number of λ_N but can be related with the integers N_1, N_W

The Ambiguity Fixing techniques take benefit of this INTEGER NATURE of N_1, N_2 ambiguities to properly fix them, reducing convergence time, and thence, achieving high accuracy quickly.

Carrier Ambiguity Fixing concept

Two different approaches can be considered:

- **Double differenced Ambiguity Fixing (e.g. RTK):**

  This is the classical approach which relies in the fact that the fractional part of carrier ambiguities cancels when forming the double differences between receivers and satellites:

  ➔ That is, given: $B_{rec}^{sat} = \lambda N_{rec}^{sat} + b_{rec} + b^{sat}$

  The double differences, regarding a reference receiver and satellite, yield: $\boxed{\Delta\nabla B_{rec}^{sat}} = B_{rec}^{sat} - B_{rec,R}^{sat} - \left(B_{rec}^{sat,R} - B_{rec,R}^{sat,R}\right) = \boxed{\lambda\,\Delta\nabla N_{rec}^{sat}}$

  where the satellite and receiver ambiguity terms (b_{rec}, b^{sat}) cancel out.

- **Absolute (or undifferenced) ambiguity fixing (e.g. PPP AR):**

Example of Ambiguity Fixing by rounding

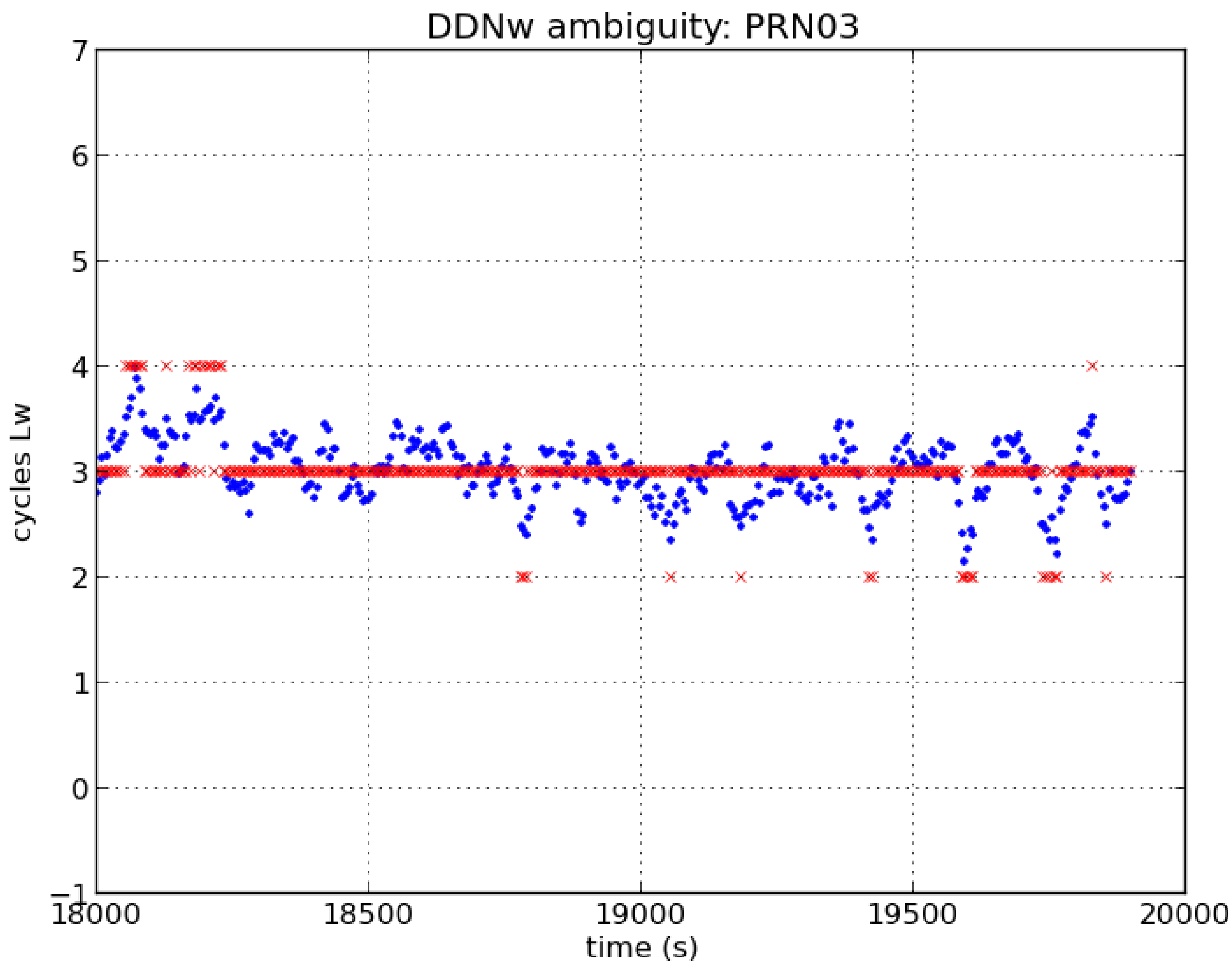

The LAMBDA METHOD

LAMBDA software package

Matlab implementation, Version 3.0

Sandra Verhagen and Bofeng Li

TUDelft Delft University of Technology

Mathematical Geodesy and Positioning, Delft University of Technology

Curtin University

Carrier Ambiguity Fixing concept

Two different approaches can be considered:

- **Double differenced Ambiguity Fixing (e.g. RTK):**

  This is the classical approach which relies in the fact that the fractional part of carrier ambiguities cancels when forming the double differences between receivers and satellites:

  ➔ That is, given: $B_{rec}^{sat} = \lambda N_{rec}^{sat} + b_{rec} + b^{sat}$

  The double differences, regarding a reference receiver and satellite, yield: $\boxed{\Delta\nabla B_{rec}^{sat}} = B_{rec}^{sat} - B_{rec,R}^{sat} - \left(B_{rec}^{sat,R} - B_{rec,R}^{sat,R} \right) = \boxed{\lambda\, \Delta\nabla N_{rec}^{sat}}$

Absolute (or undifferenced) ambiguity fixing (e.g. PPP AR):

This is a new approach, where the fractional part of the ambiguities are estimated from a global network of permanent stations and provided to the users. Thus, the user can remove this fractional part and fix the remaining ambiguity as an integer number.

$$B_{rec}^{sat} = \lambda N_{rec}^{sat} + b_{rec} + b^{sat}$$

Absolute (or undifferenced) ambiguity fixing

Nevertheless, these carrier hardware biases (or fractional part of carrier ambiguities) can be estimated together with the orbits, clocks, ionosphere and DCBs from measurements of a worldwide reference stations network.

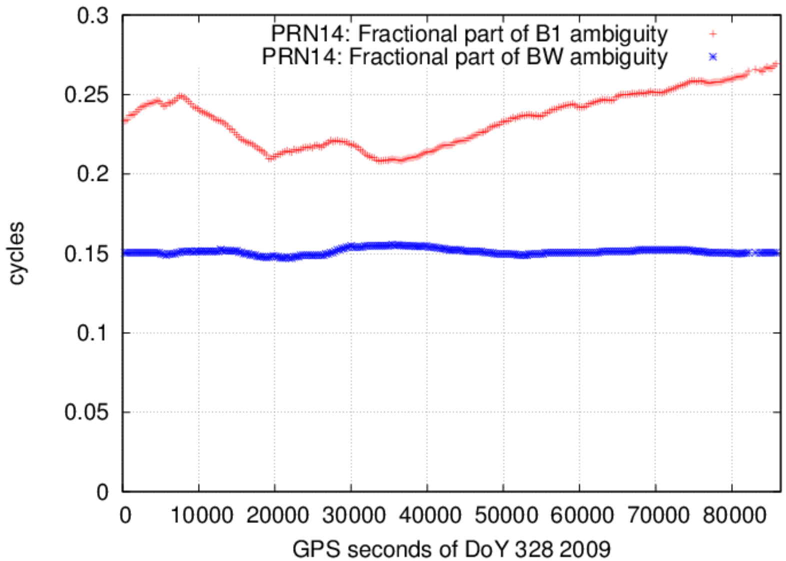

These carrier hardware biases are slow varying parameters and can be broadcast to the user, together with the other differential corrections (orbits, clocks, ionosphere…) from a reference station network.

Then, the user can remove them and estimate the remaining ambiguities as integer numbers.

This can allow world-wide PPP users to perform ambiguity fixing, without baseline length limitation, improving accuracy and reducing convergence time.

Note: These carrier hardware biases are canceled in RTK when forming Double-Differences of measurements between pairs of satellites and receivers.

June 2013

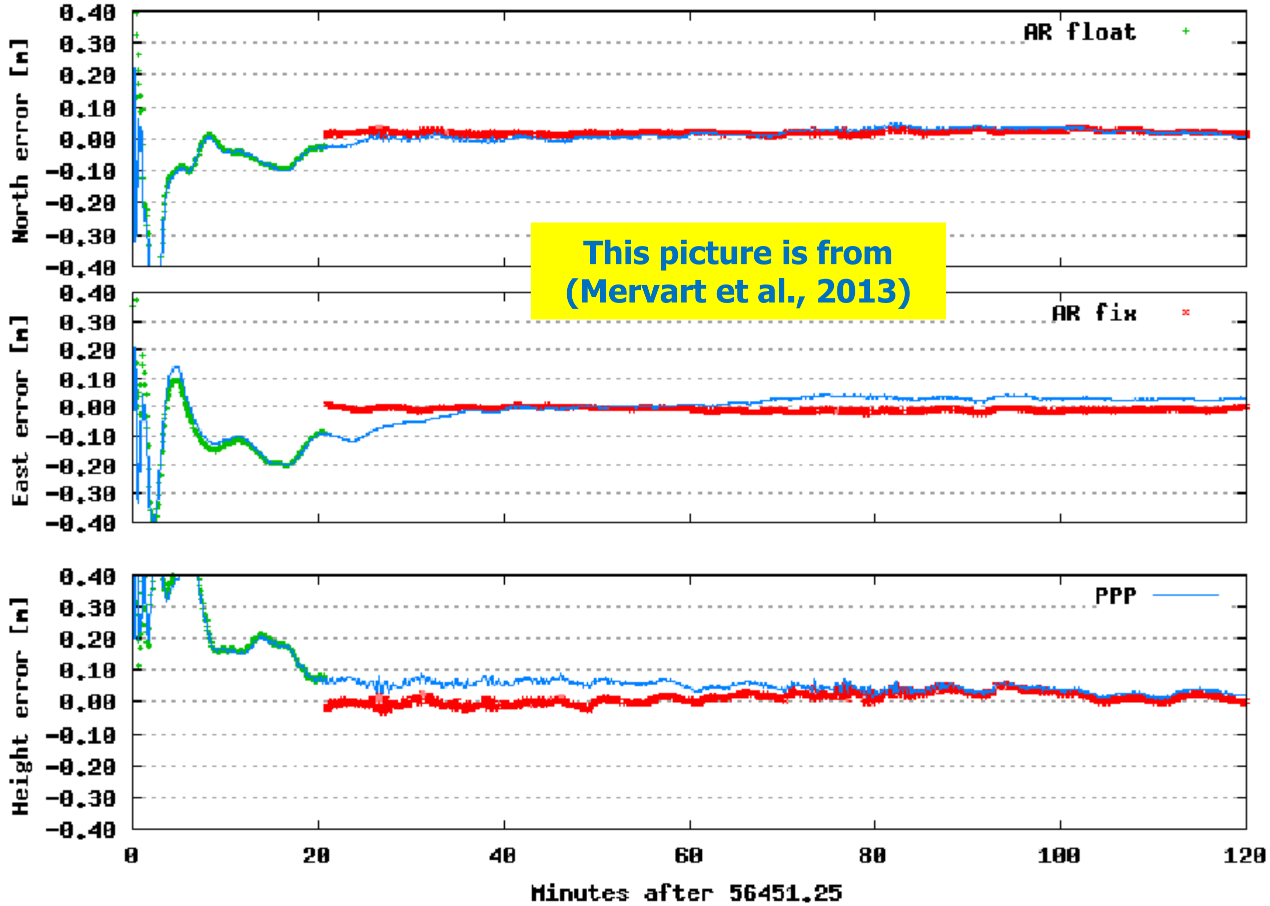

The main weakness of PPP is the large convergence time, which depend on satellites geometry, quality of data (code noise, cycle-slips…).
There is a sudden improvement when fixing carrier ambiguities, but still several tens of minutes are needed to achieve centimeter level of accuracy.

L. Mervart, C. Rocken, T. Iwabuchi, Z. Lukes and M. Kanzaki (2013). Precise Point Positioning with Fast Ambiguity Resolution – Prerequisites, Algorithms and Performance. *Proceedings of the 27th International Technical Meeting of The Satellite Division of the Institute of Navigation (ION GNSS+ 2013), Nashville, Tennessee, September 16-20, 2013.*

Contents

Precise Point Positioning (PPP)

Fast-PPP: Accelerating convergence with IONO

- During the early 2000s gAGE/UPC developed a two layers grid model, and afterwards assessed its suitability to help the PPP convergence.

These figures are from (Juan et al, 2012)

24 November 2009 (low solar activity)

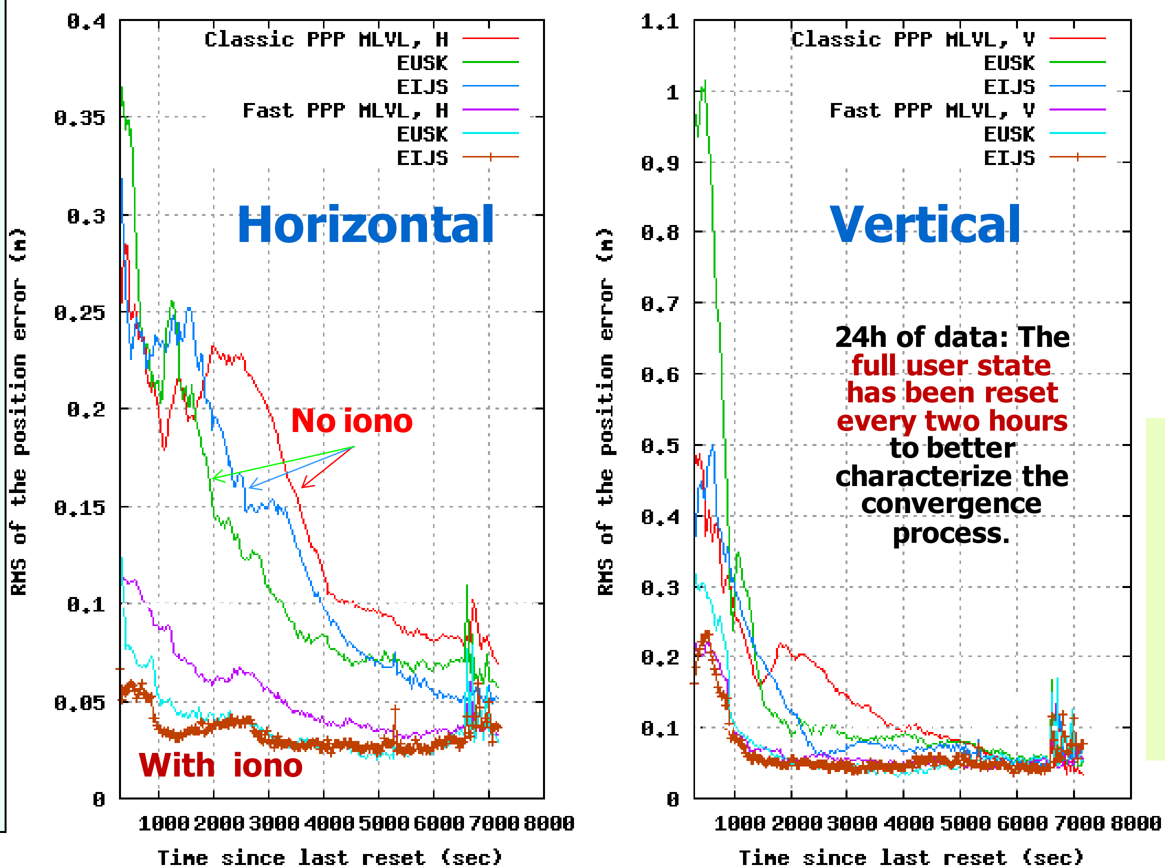

This last study was done in the context of ESA project "**Fast-PPP**" and the **technique is protected** by an **ESA patent since 2011.** (PCT/EP2011/001512)

More recently, the accurate ionospheric model has been extended to **worldwide** (Rovira, et al 2014)

MLVL (252km), EUSK (170km) and EIJS (95km)
(km from the nearest reference receiver)

Actual GNSS Data the entire Year 2014

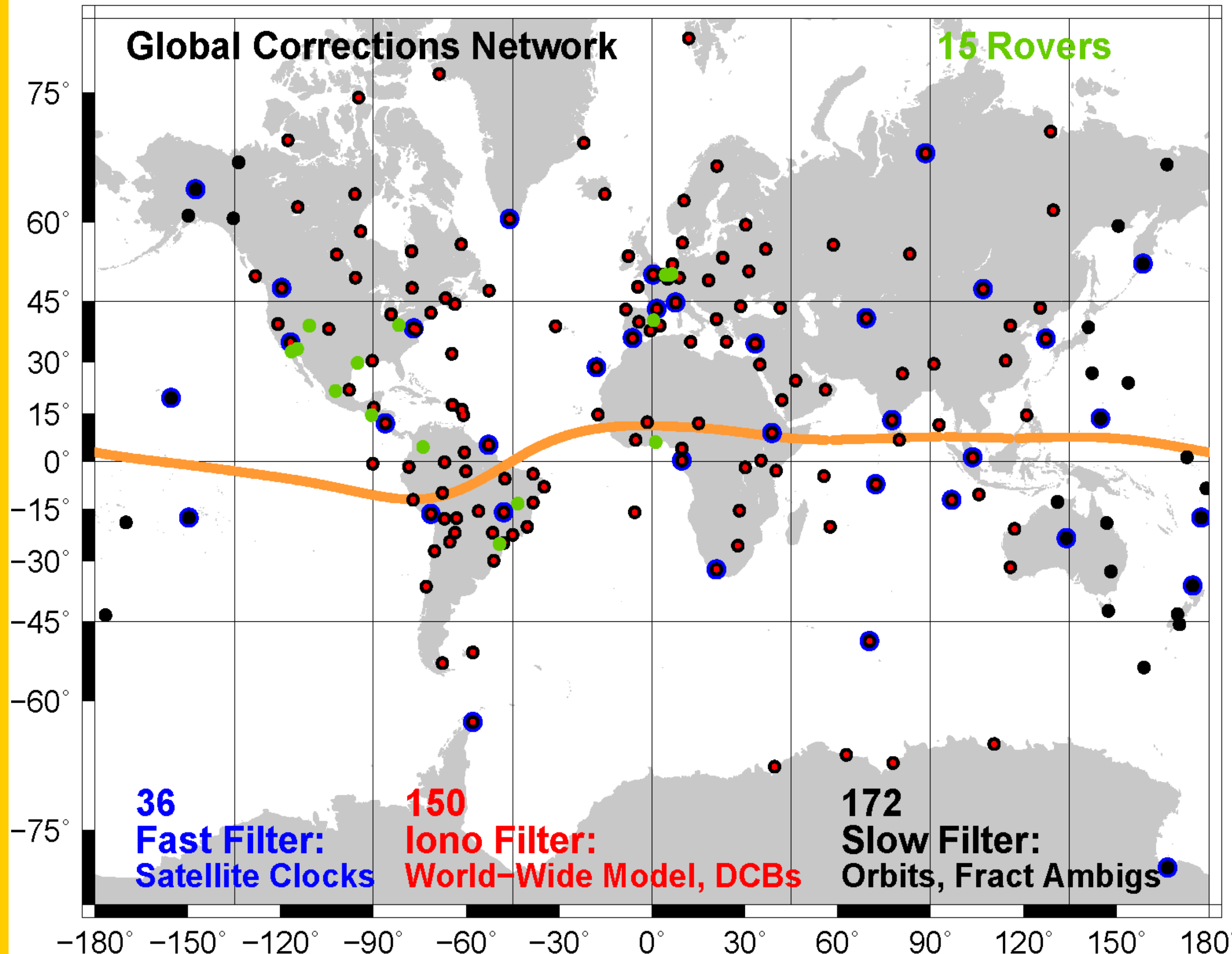

World wide Iono. model

Rovers are located at distances are orders of magnitude greater than RTK baselines

Close to maximum Solar Cycle conditions

Moderate Geomagnetic Dst Values

- ***How the ionosphere helps the filter convergence in Fast-PPP?***

➔ **In the classical PPP, the navigation filter convergence is driven by the convergence of the floated iono-free ambiguity (B_C), which, at the beginning, depends on the code noise.**

1) There is a constraint between the wide-lane ambiguity (B_w), the iono-free ambiguity (B_C) and the ionospheric refraction ($STEC$) and DCB.

$$B_C = B_W - 1.98\,(L_1 - L_2 - STEC - DCB)$$

2) The wide-lane ambiguity (B_w) is estimated/fixed quickly
(~5 minutes with 2-freq and in single epoch with 3-freq. signals).

3) The ionosphere ($STEC$) is the bridge (through the mentioned constraint) to transfer the quick accuracy achieved in the wide-lane ambiguity (B_w) computed value to the iono-free ambiguity (B_C) estimation, accelerating in this way the filter convergence.

➔ **Thence, in Fast-PPP the convergence time is strongly reduced thanks to the** quick wide-lane ambiguity fixing and the accurate ionospheric corrections. It allows to achieve High Accuracy quickly (~5 minutes with 2-freq & single epoch with 3-freq).

The ionosphere will help provided that its quality (noise/error) is better than the code

This is a conceptual approach!

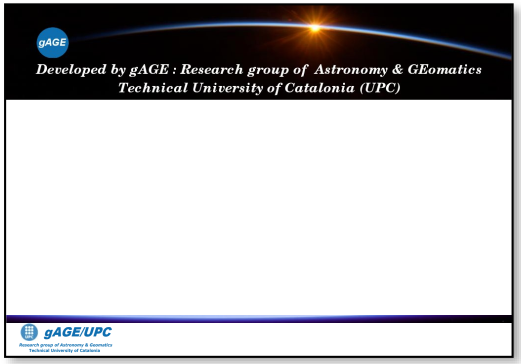

300 seconds smoothing

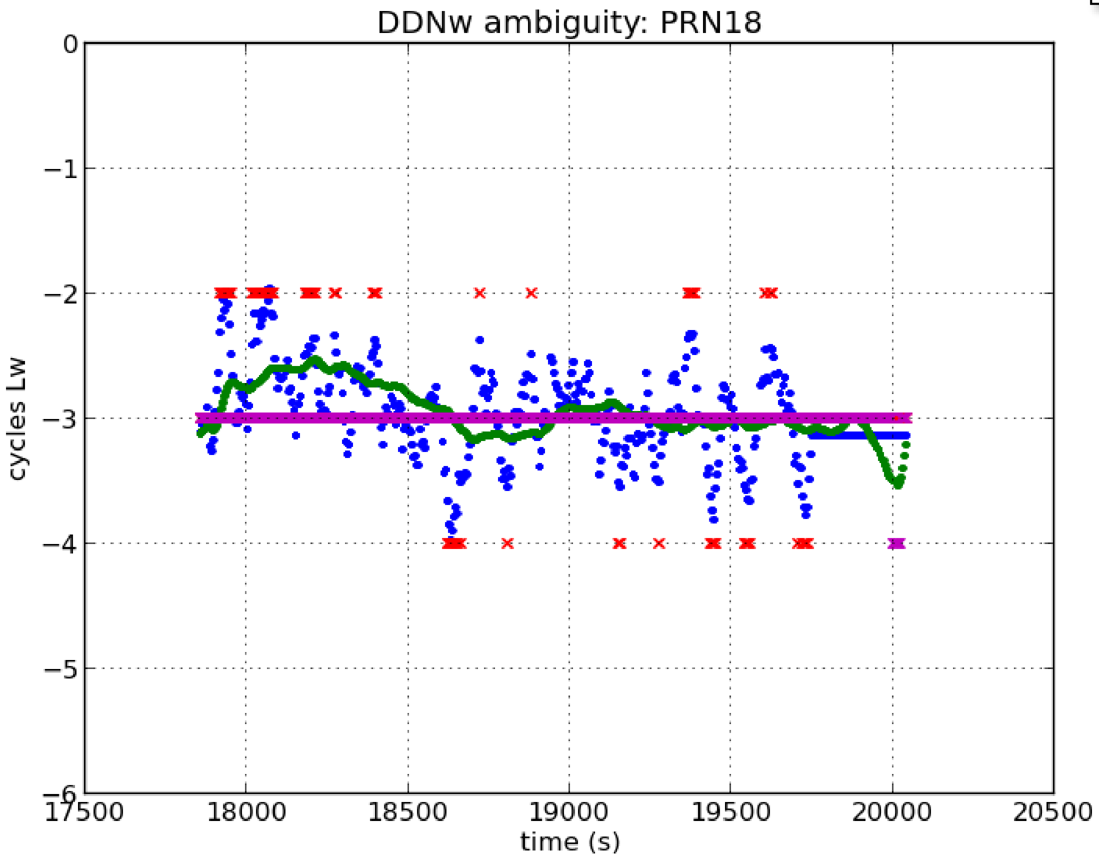

References

[RD-1] J. Sanz Subirana, J.M. Juan Zornoza, M. Hernández-Pajares, GNSS Data processing. Volume 1: Fundamentals and Algorithms. ESA TM-23/1. ESA Communications, 2013.

[RD-2] J. Sanz Subirana, J.M. Juan Zornoza, M. Hernández-Pajares, GNSS Data processing. Volume 2: Laboratory Exercises. ESA TM-23/2. ESA Communications, 2013.

[RD-3] Pratap Misra, Per Enge. Global Positioning System. Signals, Measurements, and Performance. Ganga –Jamuna Press, 2004.

[RD-4] B. Hofmann-Wellenhof et al. GPS, Theory and Practice. Springer-Verlag. Wien, New York, 1994.

[RD-5] Juan, J.M., Hernandez-Pajares, M., Sanz, J., Ramos- Bosch, P., Aragon-Angel, A., Orus, R., Ochieng, W., Feng, S., Coutinho, P., Samson, J. and Tossaint, M., 2012a. Enhanced Precise Point Positioning for GNSS Users. IEEE Transactions on Geoscience and Remote Sensing PP, issue 99, pp. 1-10.

[RD-6] Sandra Verhagen and Bofeng L., LAMBDA software package. MATLAB implementation, Version 3.0. Mathematical Geodesy and Positioning, Delft University of Technology.

[RD-7] L. Mervart, C. Rocken, T. Iwabuchi, Z. Lukes and M. Kanzaki (2013). Precise Point Positioning with Fast Ambiguity Resolution – Prerequisites, Algorithms and Performance. Proceedings of the 27th International Technical Meeting of The Satellite Division of the Institute of Navigation (ION GNSS+ 2013), Nashville, Tennessee, September 16-20, 2013.

[RD-8] Fast-PPP: International Patent Application PCT/EP2011/001512. International patent: G01S19/44 (ESA ref.: ESA/PAT/566).

[RD-9] Juan, JM., M. Hernández-Pajares, J. Sanz, P. Ramos-Bosch, A. Aragón-Àngel, R. Orús, W. Ochieng, S. Feng, M. Jofre, P. Coutinho, J. Samson, and M. Tossaint (2012). Enhanced Precise Point Positioning for GNSS Users, IEEE transactions on geoscience and remote sensing, April 2012, Issue: 99.

[RD-10] Rovira-Garcia A., Juan J. M., Sanz J., González-Casado G. (2015). "A World-Wide Ionospheric Model for Fast Precise Point Positioning", IEEE Transactions on Geoscience and Remote Sensing, Volume: 53, Issue: 8, pp 4596-4604, DOI10.1109/TGRS.2015.2402598 (Open Access).

Thank you

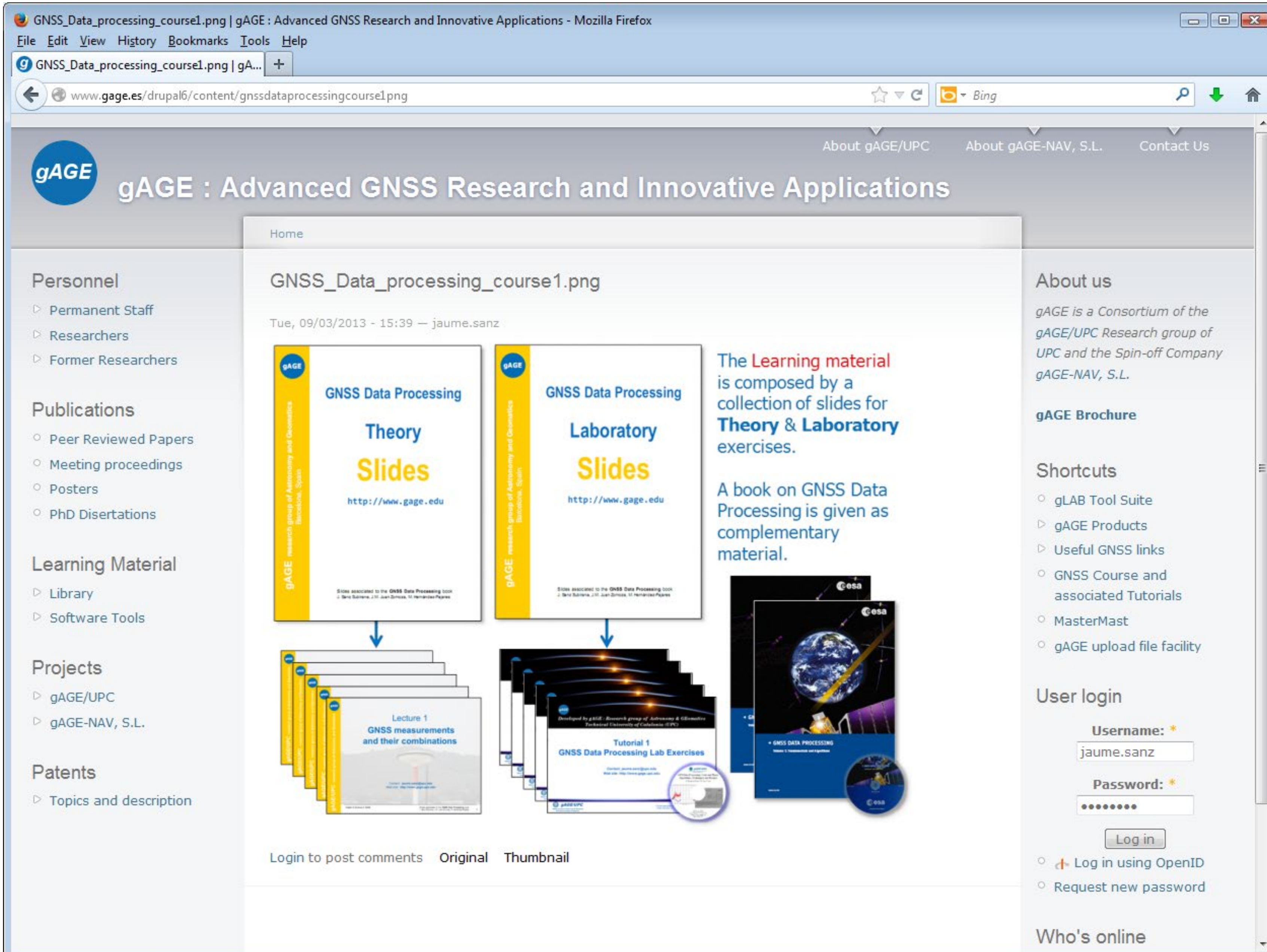
GNSS_Data_processing_course1.png | gAGE : Advanced GNSS Research and Innovative Applications - Mozilla Firefox
File Edit View History Bookmarks Tools Help
www.gage.es/drupal6/content/gnssdataprocessingcourse1png
About gAGE/UPC
About gAGE-NAV, S.L.
Contact Us
gAGE : Advanced GNSS Research and Innovative Applications
Home
Personnel
Permanent Staff
Researchers
Former Researchers
Publications
Peer Reviewed Papers
Meeting proceedings
Posters
PhD Disertations
Learning Material
Library
Software Tools
Projects
gAGE/UPC
gAGE-NAV, S.L.
Patents
Topics and description
GNSS_Data_processing_course1.png
Tue, 09/03/2013 - 15:39 — jaume.sanz
GNSS Data Processing
Theory
Slides
http://www.gage.edu
GNSS Data Processing
Laboratory
Slides
http://www.gage.edu
The Learning material is composed by a collection of slides for Theory & Laboratory exercises.
A book on GNSS Data Processing is given as complementary material.
Lecture 1
GNSS measurements and their combinations
Tutorial 1
GNSS Data Processing Lab Exercises
Login to post comments
Original
Thumbnail
About us
gAGE is a Consortium of the gAGE/UPC Research group of UPC and the Spin-off Company gAGE-NAV, S.L.
gAGE Brochure
Shortcuts
gLAB Tool Suite
gAGE Products
Useful GNSS links
GNSS Course and associated Tutorials
MasterMast
gAGE upload file facility
User login
Username: *
jaume.sanz
Password: *
Log in
Log in using OpenID
Request new password
Who's online

GNSS Data Processing, Vol. 1: Fundamentals and Algorithms.
GNSS Data Processing, Vol. 2: Laboratory exercises.

Backup slides

gAGE/UPC research group of Astronomy and Geomatics
BarcelonaTECH, Spain

Fast-PPP Ionospheric Model

technique's core

1.- Derived from the geometry-free combination of **carrier-phases:**

$$LI = L1 - L2$$

2.- Ambiguities are fixed (thanks to the CPF accurate geodetic modelling):

Unambiguous Carrier-phase noise (mm) $LI_i^j - BI_i^j = STEC_i^j + DCB_i - DCB^j$

3.- The Slant Total Electron Content (STEC) is estimated with Vertical STEC (VTEC) on each "k" Ionospheric Grid Point (IGP) at the **two-layers:**

$$STEC_i^j = \Sigma\, \alpha_k \cdot VTEC_k$$

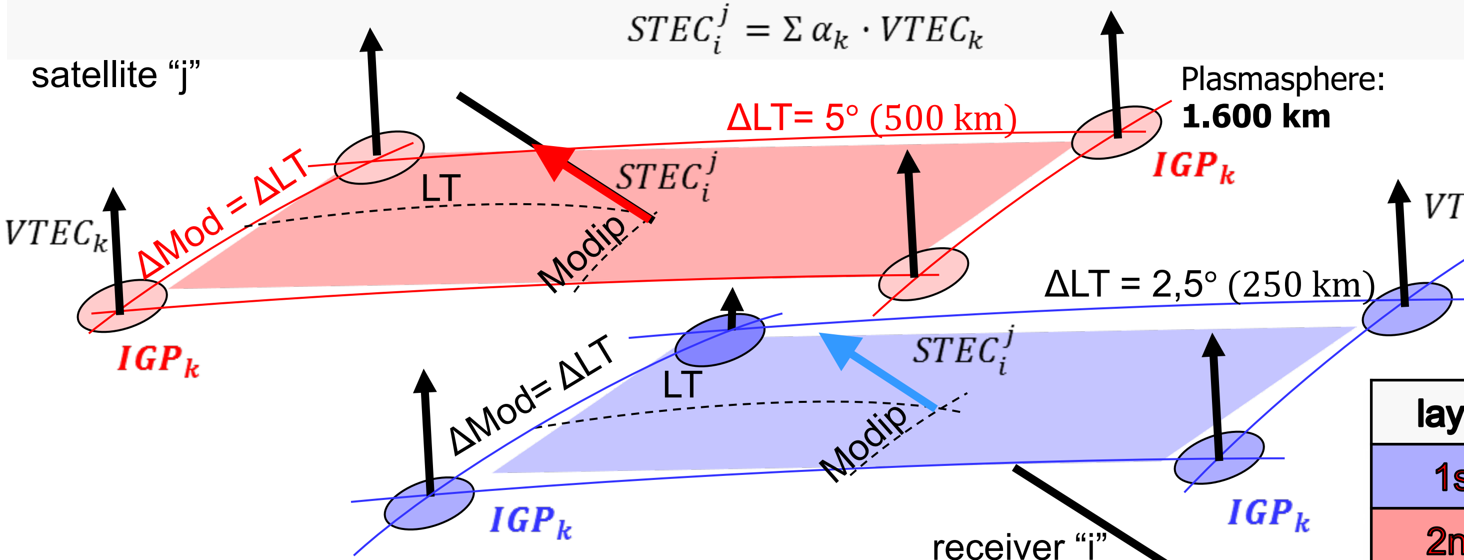

layer	IGPs
1st	7184
2nd	1800

Orbit errors (4cm) + sat Clocks (6cm)
Iono Accuracy <= 1 TECU (16 cm in L1)

2-Layer Ionospheric Maps during Storm of DoY 058-2014

2nd Layer

Plasma-sphere 1600 km

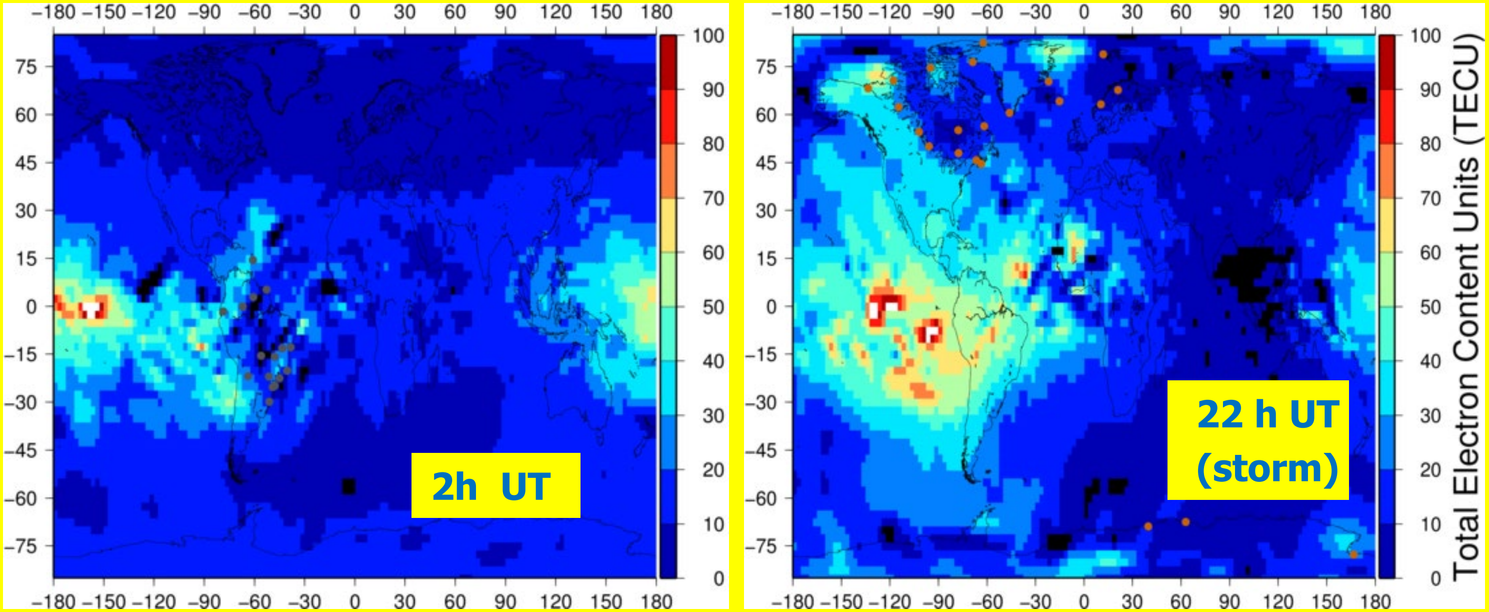

1st Layer

Iono-sphere 270 km

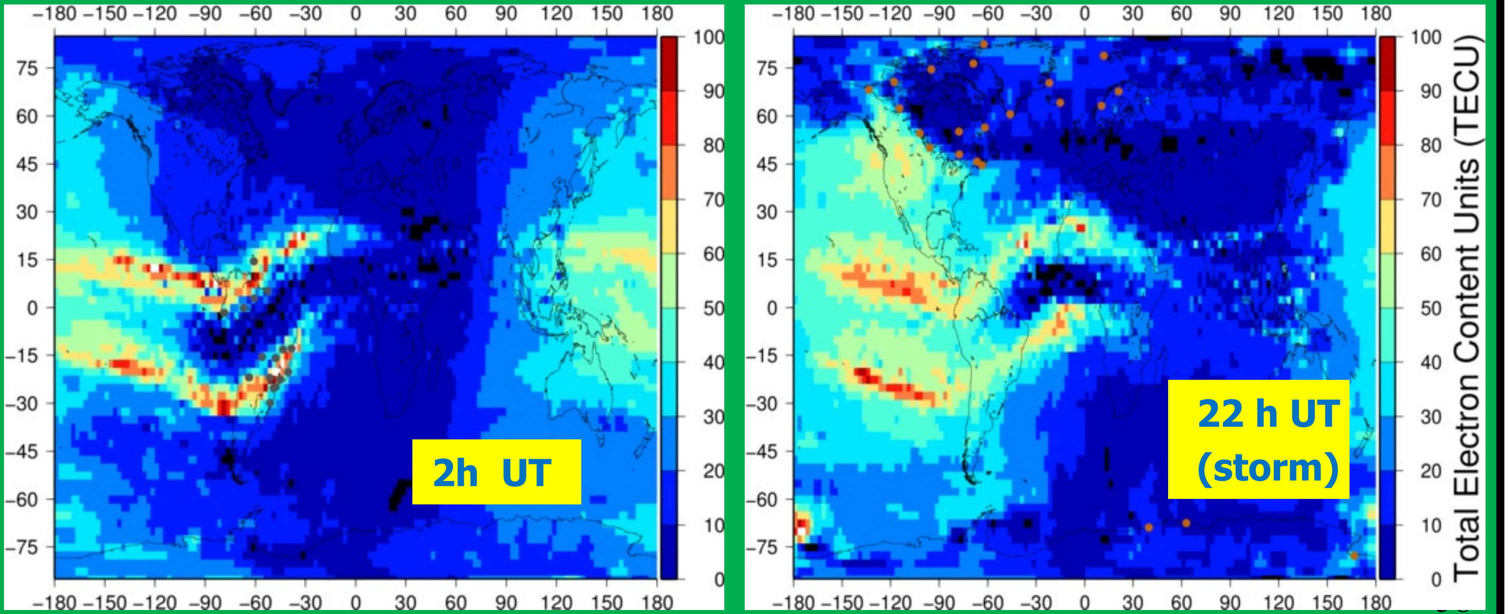

Agreement Electron Contents of dual-layers between GIM derived from "earth" data and "space-borne" data

Independent data

4 weeks of Low Earth Orbit Radio Occultations year 2007.

1 day of gAGE dual-layer GIM.

TEC ratio:

$$\frac{IonoTEC}{IonoTEC + PlasmaTEC}$$

Neglecting this effect, introduce a miss-modelling **degrading navigation.**

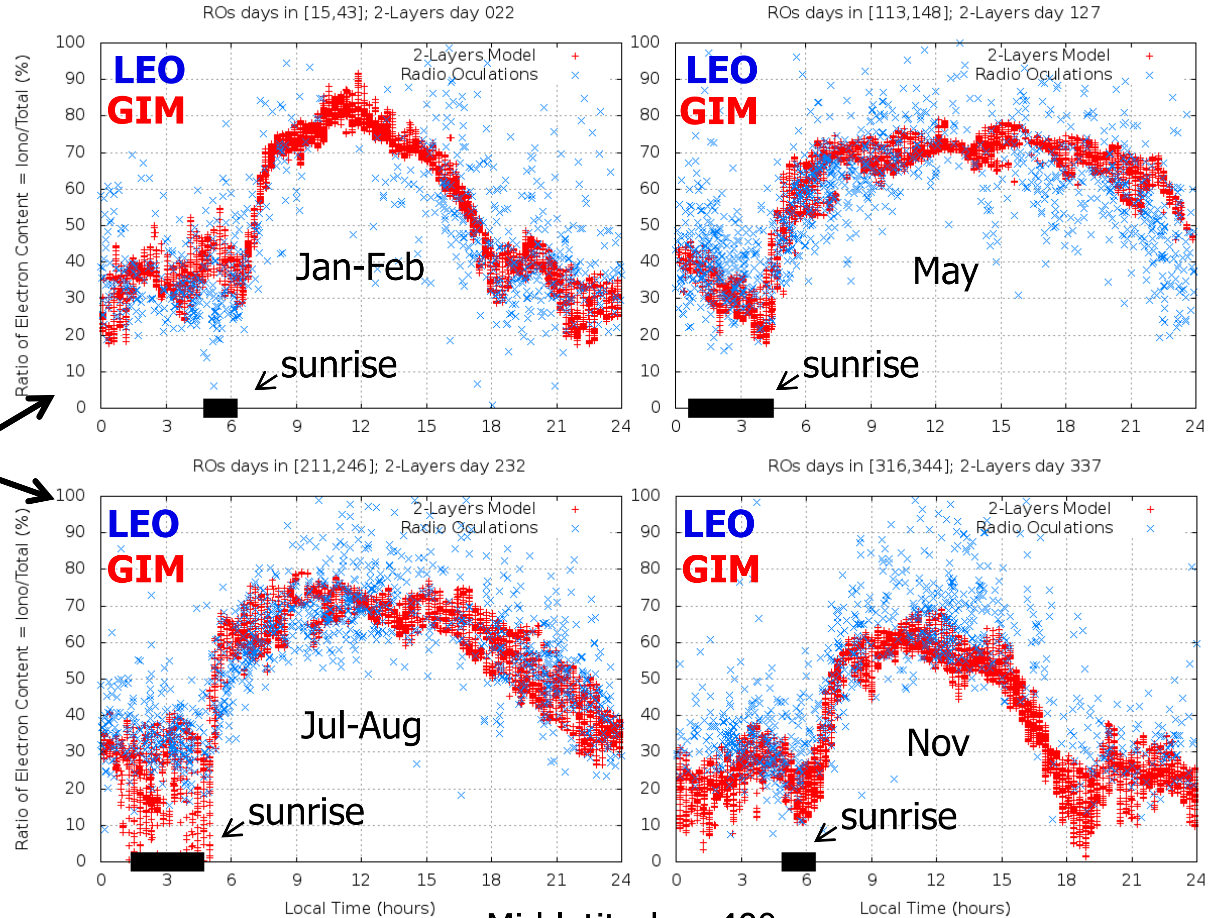

Mid latitude ~40º

G. González-Casado, J. M. Juan, J. Sanz, A. Rovira-Garcia, and A. Aragon-Angel. "**Determination of the Ionospheric and Plasmaspheric contributions to the Total Electron Content using Radio Occultations and Global Ionospheric Maps**" Journal of Geophysical Research, 101002/2014JA020807.

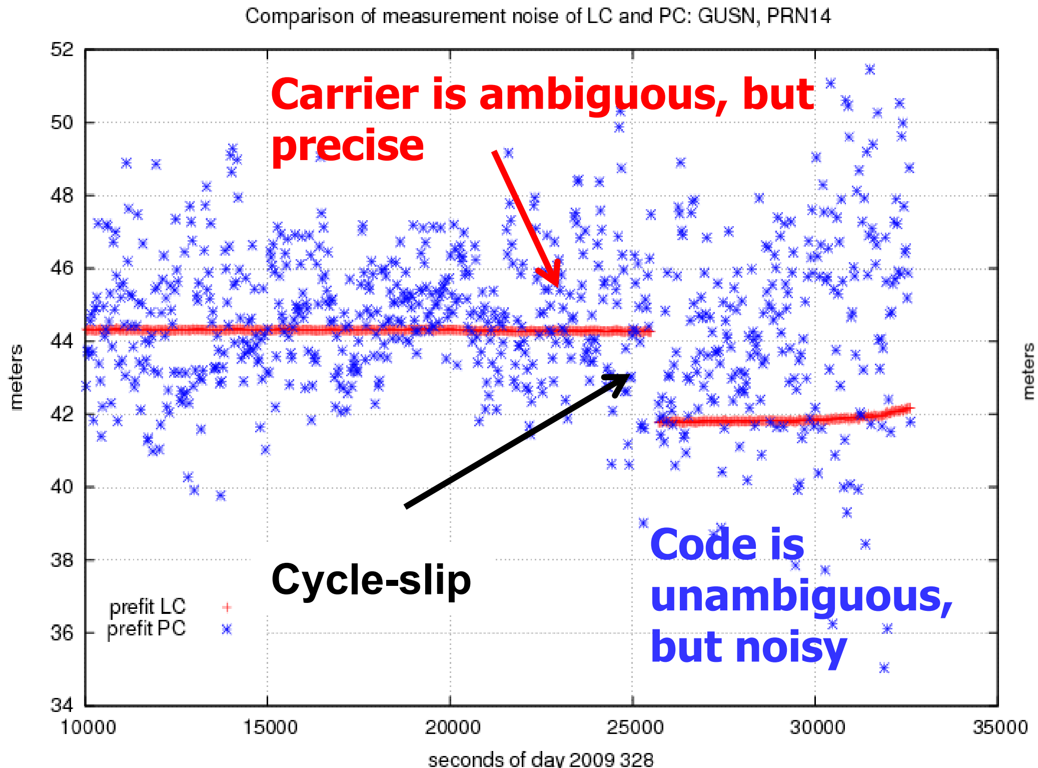

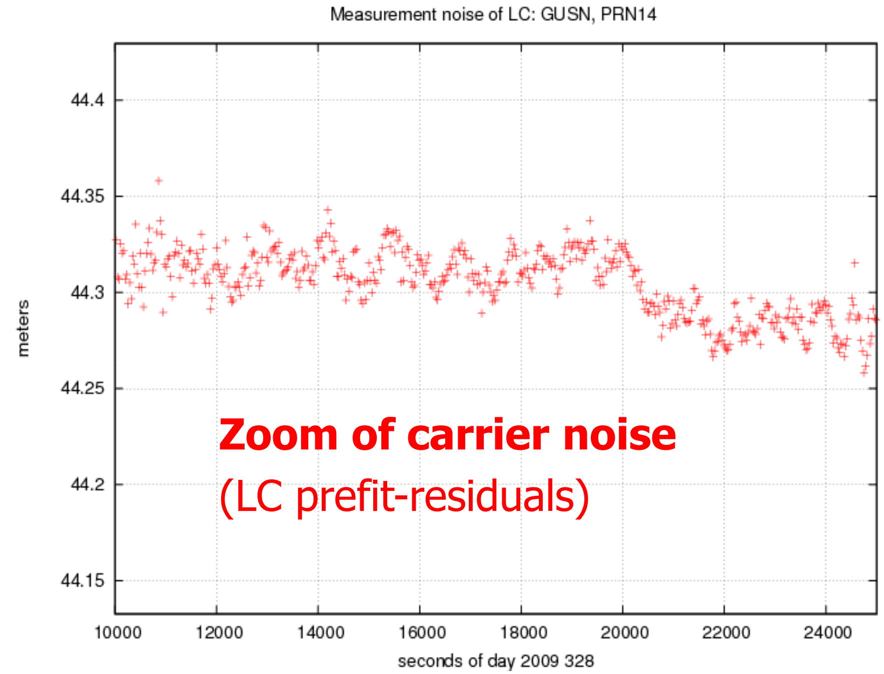

- **Code** measurements are unambiguous but noisy (meter level noise).
- **Carrier** measurements are precise (few millimetres of noise) but ambiguous (the unknown ambiguities can reach thousands of km).
- **Carrier phase ambiguities are estimated in the navigation filter** along with the other parameters (coordinates, clock offsets, etc.). If these ambiguities were fixed, measurements accurate to the level of few millimetres would be available for positioning. However, some time is needed to decorrelate such ambiguities from the other parameters in the filter, and the estimated values are not fully unbiased.

Convergence: DoYs 169-200 of 2014

6 Positioning modes per rover, resets every 2h:

a) Reference Iono-Free sol

b) Iono Sol: IONEX (IGS-GIM):

c) Iono Sol. Fast-PPP IONO:

(Close to Solar Maximum)

GRAPHIC 1F +
PPP 2F ×

IONEX 1F ✳
PPP+IONEX 2F □

Fast-PPP 1F ■
Fast-PPP 2F ☼

Rover EIJS (5ºE, 50ºN): Mid Latitude, 76 km

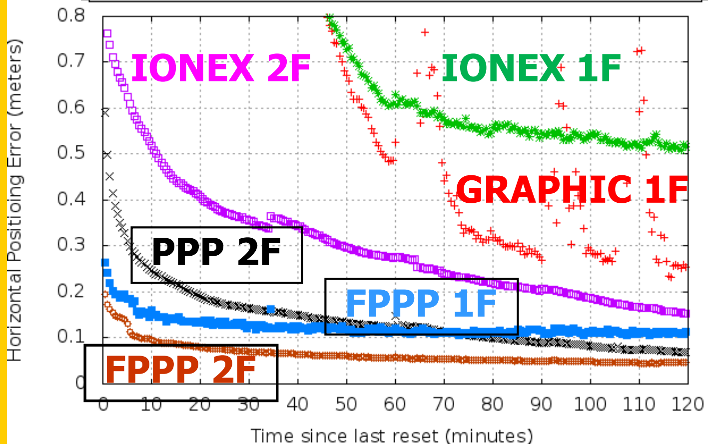

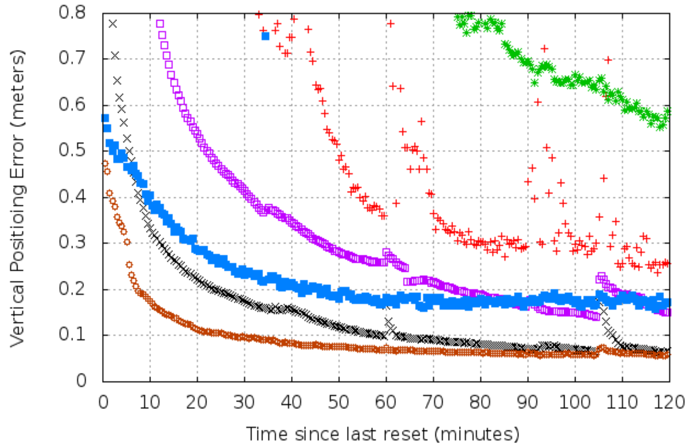

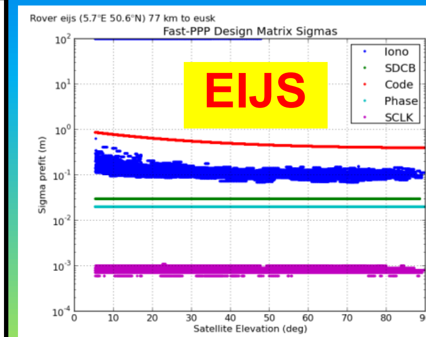

Benefits of applying external ionospheric corrections are expected, provided its quality is superior to that of code noise.

Rover LKHU (95ºW, 29ºS): Low latitude, 455 km

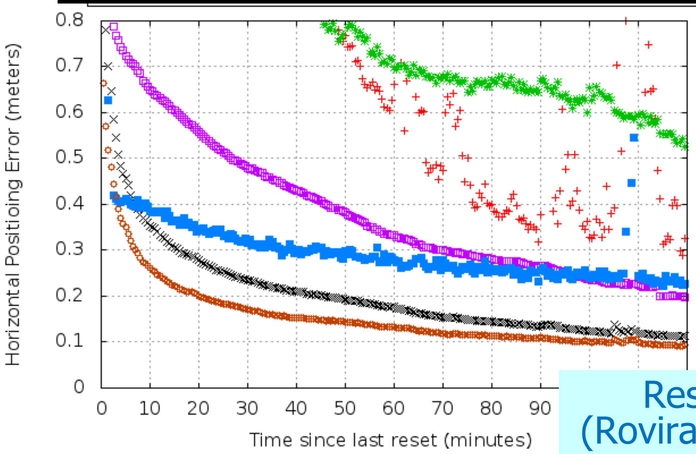

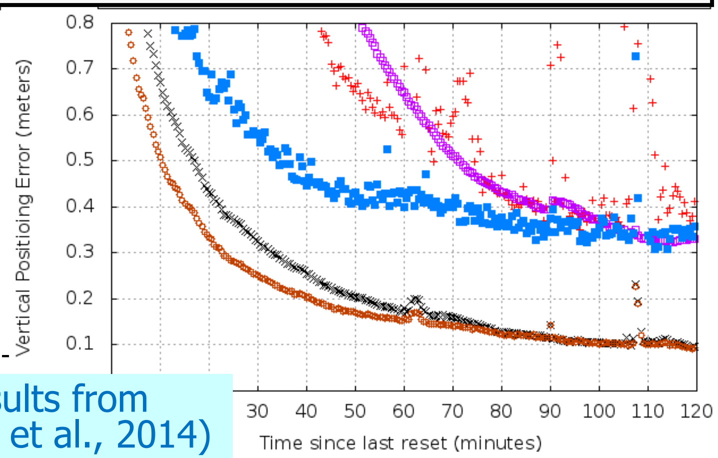

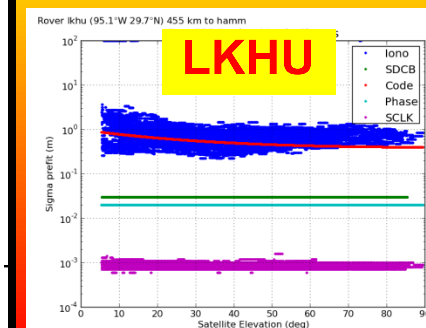

Results from (Rovira et al., 2014)